Large-Scale Distribution of CH_4 in the Western Pacific: Sources and Transport from the Asian Continent

Karen B. Bartlett[1]
Glen W. Sachse[2]
Thomas Slate[3]
Charles Harward[4]
Donald R. Blake[5]

[1]Institute for the Study of Earth, Oceans, and Space
University of New Hampshire
Durham, NH

[2]NASA Langley Research Center
Hampton, VA

[3]Swales Aerospace
Hampton, VA

[4]Science Applications International Corp.
Hampton, VA

[5]Department of Chemistry
University of California, Irvine
Irvine, CA

Submitted to
Journal of Geophysical Research

Abstract

Methane (CH_4) mixing ratios in the northern Pacific Basin were sampled from two aircraft during the TRACE-P mission (**TRA**nsport and **C**hemical **E**volution over the **P**acific) from February through early April 2001, yielding a high-resolution, high-precision data set of roughly 13,800 measurements for this chemically and radiatively important trace gas. Mixing ratios ranged between 1602 ppbv in stratospherically-influenced air and 2149 ppbv in highly polluted air. Overall, CH_4 mixing ratios were highly correlated with a variety of other trace gases characteristic of a mix of anthropogenic industrial and combustion sources and were strikingly correlated with ethane (C_2H_6) in particular. Averages with latitude in the near-surface (0-2 km) show that CH_4 was elevated well above clean, background levels north of 15^{o}N close to the Asian continent. In the central and eastern Pacific, levels of CH_4 were lower as continental inputs were mixed horizontally and vertically during transport. Overall, the correlation between CH_4 and other hydrocarbons such as ethane (C_2H_6), ethyne (C_2H_2), and propane (C_3H_8) as well as the urban/industrial tracer C_2Cl_4, suggests that for CH_4 co-located sources such as landfills, wastewater treatment, and fossil fuel use associated with urban areas dominate regional inputs at this time. Comparisons between measurements made during TRACE-P and those of PEM - West B, flown during roughly the same time of year and under a similar meteorological setting 7 years earlier, suggest that although the TRACE-P CH_4 observations are significantly higher, the changes largely parallel increases seen in background air over this time interval.

1. Introduction

The increasing industrialization occurring throughout the Asian continent has spurred a series of research efforts over the past decade, attempting to assess how these quantitative and qualitative changes in emissions have affected the global atmosphere. These efforts have included NASA's PEM West A and B missions, flown in 1991 and 1994 respectively, which examined the effects of seasonal differences in meteorology, transport, and source strengths on air quality over the Pacific Basin (see Hoell et al., 1997 for summary). The most recent research program conducted over this region is that of TRACE-P (**TRA**nsport and **C**hemical **E**volution over the **P**acific), focused on improving our understanding of how outflow from the Asian continent affects the composition of the atmosphere over the Pacific and assessing the changes that have occurred since PEM West, as rapid industrialization and increased energy usage have continued (Streets et al., this issue). TRACE-P is the latest in a long series of aircraft missions flown by NASA as part of its Global Tropospheric Experiment (GTE) which have undertaken to both characterize the natural processes controlling the chemistry of the troposphere and to determine how anthropogenic perturbations have affected this chemistry. Building on the earlier PEM West missions, TRACE-P was flown from late February - early April of 2001, when continental outflow to the Pacific Basin was expected to be near its peak due to strong westerly transport and active convection over Asia (Merrill et al., 1997). Matching the timing of TRACE-P to that of PEM - West B (February-March 1994) also provides an opportunity to compare results under similar meteorological conditions and to focus on possible changes in emissions over the intervening 7 years.

Methane (CH_4) is the most abundant atmospheric hydrocarbon, with a lifetime of roughly 9 years (Prinn et al., 1995). Although atmospheric levels of CH_4 are much lower than CO_2, the

fact that CH_4 absorbs outgoing radiation more efficiently means that change in its atmospheric significantly impacts climate change. Methane plays important radiative and chemical roles in both the troposphere and stratosphere and has undergone a variable and poorly understood increase over the last several hundred years (Dlugokencky et al., 1994, 1998; Gupta et al., 1996; Francey et al., 1999; Bräunlich et al., 2001). Sources of CH_4 are both natural and anthropogenic, and are linked to climate variables such as temperature and rainfall as well as human populations and energy usage. Ongoing changes occurring over the Asian continent in population, land use, and the quality and quantity of energy used will significantly impact the release of CH_4 (Streets et al., 2001).

Because TRACE-P was flown in the Asian spring, CH_4 emissions from natural wetlands and rice paddies, calculated to be the single largest anthropogenically-controlled source in the region (Streets et al., 2001), are expected to be near seasonal lows. Temperatures and rainfall, major controls on emissions from wetlands, are relatively low during spring and the seasonal planting of rice is just commencing (Matthews et al., 1991; Yao et al., 1996; Khalil et al., 1998). Sources of CH_4 would therefore expected to be dominated by those associated with urban and industrial centers such as landfills, wastewater treatment, and fuel usage. Also important is the release of CH_4 during biofuel and biomass burning through incomplete combustion. In more rural areas, CH_4 produced during enteric fermentation by ruminants such as cattle makes a significant contribution. Assuming paddy emissions are near zero during the TRACE-P time period, annual inventories for anthropogenic CH_4 sources compiled for China and southeast Asian nations according to IPCC guidelines for the year 2000 (Streets et al., this issue) indicate that co-located urban/industrial sources (landfills, wastewater treatment, fossil fuel usage) would

release roughly 38% of total emissions. Animal populations and coal mining, distributed more diffusely and in more rural regions, release on the order of 45%. Biomass burning, a seasonally varying source that should be beginning to decrease from its winter seasonal maximum (Hao and Liu, 1994; Cooke et al., 1996; Randriambelo et al., 2000) and biofuel burning (Brocard et al., 1998; Lelieveld et al., 2001), are estimated to contribute roughly 17%. The relative importance of various CH_4 sources varies widely between countries as well as between regions in large nations such as China, and therefore characteristic source trace gas signatures can vary widely for CH_4 depending upon individual air mass trajectories. For example, Heald et al. (this issue) suggest that biomass burning in southeast Asia over the TRACE-P period of late spring was near its seasonal peak.

In this report, we discuss a high-precision, high-resolution CH_4 data set sampled during the TRACE-P mission. Roughly 13,800 measurements, ranging from the near-surface to roughly 12 km altitude, were made and range from 1602 ppbv in stratospherically influenced air to 2149 ppbv in highly polluted air. Methane mixing ratios were highly correlated with a variety of other trace gases characteristic of a mix of industrial and combustion anthropogenic sources. Below we give a brief overview of the TRACE-P mission, followed by a description of the CH_4 sampling methodology. Section 4 describes the spatial distribution of CH_4 over the northern Pacific during TRACE-P, while section 5 compares the measurements to those made during PWB, seven years earlier under similar meteorological conditions.

2. The TRACE-P Expedition

The TRACE-P mission used two NASA aircraft, a DC-8 with a maximum sampling

altitude of about 12 km and a P-3B with a maximum sampling altitude of about 7 km, and sampled most intensely between roughly 20°N and 40°N. Flight tracks and a description of the instrumentation and its characteristics can be found in Kleb et al. (this issue). Sampling was conducted from 23 February through 9 April, 2001, slightly later by several weeks than that conducted during PEM - West B (hereafter noted as PWB), which was flown 25 January - 16 March 1994. As detailed by Fuelberg et al. (this issue), TRACE-P was flown during the transition period between air flows characteristic of winter to those of spring. The ITCZ (Intertropical Convergence Zone) was not well developed during the mission and the Japan Jet, located at about 35°N and extending west back to Africa, was relatively strong, as is typical for this time of year. Areas of widespread precipitation covered the middle latitudes of the North Pacific Basin during the mission, some in association with lightning and the rapid transport characteristic of deep convection. TRACE-P sampling occurred during neutral to weak La Nina conditions (Fuelberg et al., this issue) and flow patterns and precipitation appear to be quite similar to the meteorological conditions observed during PWB.

3. Methodology

Methane was sampled on both the DC-8 and P-3B aircraft during TRACE-P, using the DACOM I and II instruments (**D**ifferential **A**bsorption **CO** **M**easurement) respectively. These instruments are tunable diode laser systems (Sachse, 1987; 1991) which simultaneously measure CH_4, CO, and N_2O. The same instrument system was used during PWB. DACOM uses three lasers (4.7, 4.5, and 7.6 microns for CO, N_2O, and CH_4 respectively) which are combined with optical filters and directed through a 0.3 l Herriott cell containing a 36 m long optical path. After

exiting, the laser beams are spectrally isolated and directed to separate LN_2-cooled InSb and HgCdTe detectors. A wavelength reference cell containing several torr of each of the gases is used to wavelength lock each of the lasers to the appropriate absorption lines. After being drawn through a permeable membrane dryer to remove water vapor, ambient air enters the Herriott cell, the volume of which is exchanged twice a second, assuming piston flow. The Herriott cell is maintained at 100 torr to minimize potential spectral overlap from other atmospheric species. For typical ambient atmospheric levels, the absorption signal magnitudes are proportional to the mixing ratios of the three measured gases. Calibration of instrument response is performed by periodically flowing calibration gas with known near-ambient concentrations and zero air through the Herriot cell. Calibrations are performed approximately every 12 minutes with NOAA/CMDL calibration cylinders. Accuracies of the working standards are ± 1% for CH_4 and ± 2% CO. Consistency in the use of NOAA/CMDL standards on both the TRACE-P and PWB missions permits direct comparison of the samples collected on the missions, as well as with those collected as part of the CMDL clean air network.

Although CH_4 measurements are made every 5 s, we have averaged the data to 60 s to integrate with other data sampled on the aircraft. Measurement precisions for CH_4 of ± 0.15% (1 standard deviation) were obtained during TRACE-P. Methane data collected on the two aircraft are archived in their original resolution and can be obtained from the NASA-Langley Distributed Active Archive Center or through the GTE homepage (http://www-gte.larc.nasa.gov).

Instrument problems during the early part of the mission, in particular the DC-8 transit flights from Dryden CA to Kona HI (flt 4) and Kona to Guam (flt 5), prevented the collection of DACOM CH_4 data on these flights. However, whole air samples were collected by the

University of California at Irvine (UCI) for subsequent hydrocarbon and halocarbon analysis and these CH_4 data are available for some of this period. Details on sampling procedures used by the UCI group are given in Blake et al. (this issue) and Blake and Rowland (1988). Combining the UCI and DACOM CH_4 data sets however, requires cross-calibration. Using the merged 60 s data, 462 "simultaneous" samples for which there are both UCI and DACOM measurements are available from DC-8 flights 7, 8, and 9. As would be expected, these data are highly correlated, with a small number of outliers likely due to differences in sampling intervals and/or high variability in the air being sampled (Fig. 1A). However, although highly correlated, a consistent bias from a 1:1 regression line is apparent and is most likely the result of the known difference in CH_4 reference standards between NOAA/CMDL (used by DACOM) and NIST (used by UCI). Differences between simultaneous samples averaged 9 ppbv (UCI higher than DACOM) and were normally distributed, as expected for a simple calibration offset (Fig. 1B). Given the excellent correlation, the UCI data can be "normalized" to DACOM values and included with confidence for those periods during which the DACOM system was off-line.

4. Methane over the North Pacific Basin

The regional distribution of CH_4 is illustrated in Plate 1, which shows 2.5^o x 2.5^o latitude/longitude averages for all of the data, divided into three altitude ranges, a lower, well-mixed boundary layer of 0 - 2 km, the mid-troposphere of 2 - 6 km, and the upper troposphere, above 6 km. Because CH_4 sources are almost exclusively located on the continents and are greater in the Northern Hemisphere, mixing ratios would be expected to decrease with increasing altitude, with distance offshore, and with decreasing latitude. In addition to these general trends

seen in the TRACE-P data set, Plate 1 clearly demonstrates the elevated mixing ratios extending over a broad range of latitudes off the Asian continent as material is transported from Asia and further west into the basin. Concentrations decrease as long-lived trace gases such as CH_4 are moved away from source regions, and inputs are mixed vertically and horizontally at relatively rapid rates compared to photochemical loss. We can divide the area sampled during TRACE-P longitudinally to examine these trends as continental outflow is advected across the North Pacific Basin by the dominant westerly flow (Fuelberg et al., this issue). Here, we break the region into two longitudinal classes, the Western Pacific, ranging from the coast of the Asian continent to 160°E, and the Central/Eastern Pacific, from 160°E to the North American coast. As Plate 1 illustrates, the sampling effort during TRACE-P was concentrated largely within the Western Pacific class, and the majority of the data from the Central/Eastern Pacific class was obtained during transit flights.

One of the primary concerns when characterizing the distribution of an environmental variable like CH_4 sampled over a large area such as the Pacific is evaluating how representative the intensive, but relatively brief sampling is of the regional distribution. This evaluation is particularly critical if the derived distributions are to be compared to other times or areas. As detailed in Jacob et al. (this issue), flights conducted during TRACE-P and other similar aircraft missions were designed to meet a variety of objectives, only one of which is a regional characterization. One way to approach this problem is to compare the sampled three-dimensional distributions with those derived from models, integrated on a variety of temporal and spatial scales (see Bey et al., this issue; Schultz et al., this issue). The representativeness of sampled distributions based on the much sparcer PWA and PWB data sets has been examined in

some detail by Ehhalt et al. (1997), who concluded that the distributions were reasonable descriptions of the "true" average pattern of concentrations, despite incomplete and irregular sampling. Although clearly every aircraft mission differs, the use of two aircraft and the much more geographically extensive sampling performed during TRACE-P suggest that the derived distributions, as shown in Plate 1, are an adequate representation of true geographic patterns over the sampling period.

Averages shown in Plate 1 include the entire data set and therefore include observations which were affected by inputs from the stratosphere. Although most frequently seen at altitudes above 6 km and latitudes above 35^{o}N, stratospherically-impacted air was observed at a variety of locations throughout the mission and serves as a mechanism introducing very low CH_4 mixing ratios to the troposphere (Browell et al., this issue). These significantly lower mixing ratios, however, can mask the variability due to mixing and transport that is the focus of TRACE-P. For this reason, we have elected to remove observations identified as having significant stratospheric inputs from subsequent analysis. As shown in Figure 2, air with a significant stratospheric component has a distinctive signature, with elevated O_3 and low CH_4 and CO, among other trace gases. Here, we removed from further analysis all observations with low CH_4 and O_3 levels greater than about 100 ppbv, or with CH_4/O_3 ratios less than about 20, a total of about 450 observations. These values form a well defined group that overlaps the distribution of mixing ratios at upper altitudes but is distinct (Figure 3).

4.1 Variability with Latitude

Methane exhibits a well-known, seasonally varying latitudinal trend in background surface-level mixing ratios, from high values in the Northern Hemisphere to lower levels in the

Southern Hemisphere (Dlugokencky et al., 1994). Derived from clean air sampling at Climate Monitoring and Diagnostic Laboratory (CMDL) ground-level sites, these measurements provide a way to estimate enhancements due to Asian outflow. As shown in Figure 4A, Western Pacific average CH_4 mixing ratios in the lower 2 km are elevated well above Pacific Basin CMDL background levels north of 15°N; enhancements that range between 38 and 27 ppbv. The largest differences between CMDL background levels and those sampled in the Western Pacific are between 15° and 20°N and 30° and 35°N, reflecting outflow from Hong Kong and Japan. Averages to the south, between the equator and 15°N, were comparable to CMDL site values. At higher altitudes, mixing ratios are lower than surface background values and decrease with increasing altitude by a variable amount. Note that low, relatively constant concentrations extend from 25° to 5°N above 6 km, from roughly 15° to 5°N at 2-6 km, and are absent in the near-surface; differences reflecting the mixing of northern and southern hemispheric air at upper altitudes and the northward penetration of southern hemispheric air with characteristically lower mixing ratios of many trace gases. The air south of 25°N and at altitudes > 6 km averaged CO levels between 75 and 100 ppbv, mean C_2Cl_4 mixing ratios of ~ 2.4 pptv, and C_2H_2/CO ratios of 0.9 - 1.3. Latitudinal distributions for a variety of other trace gases including C_2H_6, C_2H_2, C_3H_8, and C_2Cl_4 were similar to those for CH_4.

At Central/Eastern Pacific longitudes (Fig. 4B), near-surface average CH_4 mixing ratios are much lower, and are similar to CMDL background values. They are between 40 and 18 ppbv lower than Western Pacific averages, with greatest differences to the north and decreasing southward. Average mixing ratios above 6 km, however, are indistinguishable from those at 2 - 6 km between the latitudes of 25° to 35°N and are actually roughly 10 ppbv higher than averages

at these latitudes in the Western Pacific. These higher concentrations of CH_4 are seen in the bottom panel of Plate 1 between 160° and roughly 180°E and are associated with enhanced CO, C_2H_6, CH_3Cl, and C_2Cl_4, among other gases. Coinciding with the most intense position of the Japan Jet (Fuelberg et al., this issue), these continental emissions appear to be rapidly and efficiently carried at altitude to the Central Pacific.

4.2 Variability with Longitude

Because CH_4 changes systematically with latitude, any longitudinal trends must account for this known source of variability. We have therefore grouped the TRACE-P observations into latitude classes, which largely correspond to trajectory-based source region classes developed during the PWB mission, Continental North (> 20°N) and Continental South (< 20°N) (Talbot et al., 1997). The three TRACE-P latitude classes, South (< 20°N, actually 7°N - 20°N), Mid (20°N - 40°N), and North (> 40°N, actually 40°N - 46°N), subdivide the PWB Continental North group to permit examination of the most intensely sampled TRACE-P region. As shown in Figure 5A, data from the North latitude class are spatially sparse and suggest only that mixing ratios fall offshore. At latitudes south of 20°N (Fig. 5C), concentrations close to the Asian continent are elevated in the near-surface only and decrease to CMDL background levels beyond 140°E. Five-day back trajectories for the data used in these averages indicates that those in the near-surface between 110° and 140°E are predominantly from the north and west over central Asia, and China, while those above 2 km are dominated by oceanic pathways, more southerly flows from southeast Asia, or westerly flow extending back to India or Africa. These general trends are in agreement with those reported in Bey et al. (2001), based on modeling PWB data.

Between 20° and 40°N, elevated CH_4 is most clearly seen below 6 km and extends to

roughly 160°E before sharply falling (Fig. 5B). Higher concentrations are also seen off the North American coast at all altitudes. If a typical average mid-Pacific mixing ratio in the near-surface is taken to be about 1770 ppbv (Fig. 5B), levels below 2 km and west of 160°E, the Western Pacific longitude class, have been increased roughly 60 ppbv due to continental inputs. At altitudes between 2 and 6 km, averages have been increased on the order of 30 ppbv. Strong longitudinal trends are also seen in averages for other trace gases, a subset of which are shown in Figure 6. Trends in CH_4 are particularly well correlated with those of other hydrocarbons such as ethane (C_2H_6; Fig. 6B), ethyne (C_2H_2; Fig. 6C), and propane (C_3H_8; data not shown). Longitudinal variation in CO (Fig. 6A) is similar to CH_4 but shows only modest elevation off the coast of North America. Note that the trends in C_2H_2 are more similar to those for CO as would be expected, since emission ratios for these gases from all types of combustion are very similar (Blake et al., 1996).

More clearly shown in Figures 5 and 6 are the enhanced levels of CH_4 and other gases above 6 km in the central Pacific discussed in Section 4.1. Average C_2H_2/CO and C_3H_8/C_2H_6 ratios, indicators of photochemical processing and mixing, and therefore the relative age of an air mass (McKeen et al., 1996; Parrish et al., 1992; Gregory et al., 1997), are both elevated in this region and range from 2.3-2.5 and from 0.12-0.13, suggesting that roughly 2 or 3 days have elapsed since emission. The use of tracers such as C_2Cl_4, indicative of urban and industrial sources (Blake et al., 1997; Wang et al., 1995), and CH_3Cl, produced predominantly during biomass burning (Rasmussen et al., 1980; Blake et al., 1996) can help clarify origins of these increased levels at high altitude. Based on these tracers (Fig.s 6D and E), elevated levels of trace gases in the Western Pacific longitudes have a variety of sources, as might be expected, with

large enhancements in both compounds. At high altitudes over the central Pacific however, C_2Cl_4 is not particularly high and CH_3Cl is strongly enhanced, suggesting that emissions from biomass burning or the burning of biofuels may be the primary source. Five-day back trajectories show that most of this air passed across southeast Asia, southern China, and northern India where significant biomass and biofuel burning occurs (Heald et al., this issue; Lelieveld et al., 2001).

A regional characterization of the North Pacific Basin during TRACE-P for selected trace gases is summarized in Table 1 for the three altitude classes (0-2 km, 2-6 km, and >6 km), the three latitudinal classes (< 20°N, 20° - 40°N, and > 40°N), and the two longitudinal classes (110° - 160°E and 160° - 240°E).

4.3 Variability with Altitude

In the preceding sections, we have used large altitude classes to group and discuss two-dimensional spatial trends. In this section, we examine trends with altitude more closely within the more intensely sampled West Pacific and contrast them with those from the Central/East Pacific. As shown in Figure 7A, average CH_4 mixing ratios at latitudes south of 20°N are relatively constant above roughly 4 km and increase sharply below. Between the latitudes of 20°N and 40°N, averaged CH_4 levels are high and increase smoothly throughout the air column. Mixing ratios are comparable to those south of 20°N only at altitudes above 9 km. In the Central/ Eastern Pacific (Figure 7F), near-surface concentrations are lower than those in the West, and decreases from the surface to altitudes of approximately 4 km are seen at all latitudes below 40°N. At more southerly latitudes, this decrease continues through the maximum altitudes sampled. However, for latitudes between 20°N and 40°N, CH_4 is elevated between the altitudes of 4 and 10 km. Altitude trends in CH_4 are strikingly correlated with a variety of other trace

gases, most notedly those of C_2H_6 (Fig. 7B and G) and C_2Cl_4, which has sources that are specific to urban/industrial activities such as dry cleaning and industrial degreasing (Fig. 7C and H). Although correlations are slightly higher over the Western Pacific, the coefficient of determination (r^2) between these spatially averaged CH_4 and C_2H_6 mixing ratios is 0.97 and for CH_4 and C_2Cl_4 is 0.92 (n=63). The slope of the regression line with C_2H_6 ($\Delta CH_4/\Delta C_2H_6$) is 0.05 ppbv/pptv and with C_2Cl_4 is 7.37 ppbv/pptv. Although the relationship with CO is not as tight (r^2=0.81; n=65), correlation between the two is still excellent overall, with a CH_4:CO regression slope of 0.58, suggesting a mixture of urban ($\Delta CH_4/\Delta CO$ ~1; Bartlett et al., 1996) and combustion sources ($\Delta CH_4/\Delta CO$ ~0.1; Scholes et al., 1996; Bartlett et al., 1996; Ferek et al., 1998). Emissions of C_2H_6, largely from the Northern Hemisphere, are believed to be dominated by natural gas losses and biomass burning (Rudolph, 1995). The tight correlation between C_2H_6 and CH_4 would indicate that these sources also predominate for CH_4 during TRACE-P.

We can further breakdown the Western Pacific longitude class to examine trends in more detail close to the Asian continent. As demonstrated in Figure 8 for 20° longitude means, there is clear coherence between average altitude profiles of all the hydrocarbons shown. Elevated CH_4 is generally confined to altitudes < 4 km west of 120°E. As air is carried away from the Asian continent, near-surface levels tend to decrease and those at high altitudes tend to increase as mixing takes place vertically and horizontally. Regression slopes between CH_4 and C_2H_6 ($\Delta CH_4/\Delta C_2H_6$) vary from 0.12 ($r^2$=0.96) in the lower 4 km west of 120°E, to 0.050 - 0.052 ppbv/pptv (120° - 140°E and 140° - 160°E). Although high throughout the region, the slope of propane to ethane ($\Delta C_3H_8/\Delta C_2H_6$) decreases in a consistent west-to-east pattern; 0.51 (< 4 km, west of 120°E), 0.44 (120° - 140°E), 0.44 (140° - 160°E), and 0.35 (160° - 180°E) as air masses

begin to age and the shorter lived propane is mixed and photochemically oxidized.

4.4 Plumes and Case Studies

High correlations between CH_4 and urban/industrial tracers such as C_2Cl_4, and the striking correspondence between hydrocarbon species suggest that the entire northern Pacific region is dominated by these sources during the late February - early April period sampled by TRACE-P. There were however, air masses sampled that had a variety of trace gas signatures since spatial heterogeneity for sources is high. In this section, we examine selected examples of elevated trace gases to investigate source variability in somewhat more detail. Correlations between selected species for several plumes are summarized in Table 2.

Some of the highest CH_4 mixing ratios sampled during TRACE-P were seen during the DC-8 flight 13 when the aircraft intercepted highly polluted air from the Shanghai area over a period of roughly 50 min. (Figure 9). Methane levels range up to 1983 ppbv within this air mass and average 1866 ppbv. Finer resolution data using the original 5 s sampling interval capture higher and more variable mixing ratios. Enhanced levels are correlated with a variety of other species including CO ($\Delta CH_4/\Delta CO$=0.22; r^2=0.90), C_2H_6 ($\Delta CH_4/\Delta C_2H_6$=0.052 ppbv/pptv; r^2=0.84), C_2H_2 ($\Delta CH_4/\Delta C_2H_2$=0.021 ppbv/pptv; r^2=0.81), C_3H_8 ($\Delta CH_4/\Delta C_3H_8$=0.052 ppbv/pptv; r^2=0.73), C_2Cl_4 ($\Delta CH_4/\Delta C_2Cl_4$=1.65 ppbv/pptv; r^2=0.73), and CH_3Cl ($\Delta CH_4/\Delta CH_3Cl$=0.155 ppbv/pptv; r^2=0.81); suggesting a complex mixture of co-located combustion, industrial, and fossil fuel sources. Because levels of CH_3Cl are extremely high (up to 1677 pptv) and the $\Delta CH_4/\Delta CO$ is relatively low, combustion inputs appear to have been sizable. Carbon monoxide is also well correlated with CH_3Cl and regression yields a relatively high emission ratio ($\Delta CH_3Cl/\Delta CO$=1.24 pptv/ppbv; r^2=0.85), but one consistent with those reported by Lobert et al.

(1991), Blake et al. (1996), and Andreae et al. (1996), particularly for smoldering combustion. Since the source area of Shanghai is highly urban, biofuel combustion (in cookstoves or for domestic heating, for example) rather than biomass burning may be the most likely combustion source.

Two distinctly different air masses were sampled during DC-8 flight 10, while flying in the vicinity of Hong Kong (Figure 10). Below approximately 4 km, Asian outflow with elevated C_2Cl_4, CO, CH_4, and other hydrocarbons was observed. Over the course of the flight, the aircraft repeated intercepted this air mass as a series of spirals were performed. Methane mixing ratios average 1818 ppbv, range up to 1883 ppbv, and are well correlated with a variety of trace gases with anthropogenic sources (Table 2). Five-day back trajectories indicate that this low-level air mass had crossed China from the north and west, after leaving northern Europe and Russia. Above about 4 km, levels of CH_3Cl are elevated (Figure 10), suggesting combustion inputs, and back trajectories indicate that this relatively well-aged air passed across southeast Asia and regions to the west as far as India and Africa. The average C_2H_2/CO and C_3H_8/C_2H_6 values in this air mass were significantly lower than those below 4 km (1.58 vs. 2.67 pptv/ppbv, and 0.12 vs. 0.29 respectively), indicating that it was at least several days older. The slope of CH_3Cl relative to CO ($\Delta CH_3Cl/\Delta CO$) above 4 km is 0.95 pptv/ppbv (r^2=0.69), consistent with biomass burning values for combustion with a significant smoldering component (Andreae et al., 1996; Blake et al., 1996). Although also statistically significant, the $\Delta CH_3Cl/\Delta CO$ slope in the near-surface air mass is much lower (0.26 pptv/ppbv; r^2=0.67). Consistent with the lower CH_3Cl inputs in near-surface air, the calculated $\Delta CH_4/\Delta CH_3Cl$ is higher than in air above 4 km (1.20 ppbv/pptv; r^2=0.43, as compared to 0.33; r^2=0.41), even though $\Delta CH_4/\Delta CO$ values are quite

similar (Table 2).

Samples collected during P-3B flight 9 in the Hong Kong area were made a variety of polluted air masses (Figure 11). At higher altitudes, the aircraft intercepted air of largely tropical origin at several locations, with low trace gas mixing ratios (average CO=77 ppbv; average CH_4=1746 ppbv; average C_2H_2/CO=0.92). Close to the surface, an air mass with high C_2Cl_4 but very little CH_3Cl was sampled, suggesting little combustion input (Figure 11A). This layer has 5-day trajectories extending back to the north and west over China and into Siberia and is characterized by elevated CO, CH_4, and other hydrocarbons (average CH_4=1822 ppbv; average C_2H_6=1877 pptv; average C_2Cl_4=8.9 pptv; average CH_3Cl=569 pptv; average C_3H_8/C_2H_6=0.29). The majority of the air sampled during the flight is polluted with a complex mixture of urban/industrial and combustion sources with source trajectories generally from the southwest across southern China, northern southeast Asia and extending back to India and Africa. Both C_2Cl_4 and CH_3Cl are enhanced (averaging 4.7 and 630 pptv respectively), as well as a suite of trace gases, and C_3H_8/C_2H_6 ratios average 0.14, suggesting that at least several days had elapsed since emission (Figure 11B).

During the P-3B transit flight 6 from Kona, Hawaii to Wake Island on 27 February, an extremely thin, well-defined polluted layer was noted at approximately 3 km. The aircraft intercepted this layer repeated over the entire flight path, suggesting that it was present over a large geographic region. This air mass is characterized by enhanced levels of both CH_3Cl (averaging 623 pptv), as well as C_2Cl_4 (averaging 5.1 pptv), and had 5 day back trajectories extending back over Japan and into China (Figure 12). The calculated $\Delta CH_4/\Delta CO$ for this air mass is 0.33, and is consistent with combustion emission ratios. At altitudes of 5 - 6 km, the

maximum altitude sampled by the aircraft, relatively clean air with largely tropical oceanic back trajectories was observed, with low CO (average=84 ppbv), CH_4 (average=1693 ppbv), and other trace gases (Figure 12A). Dominating the near-surface altitudes sampled and mixing into the relatively clean air is an air mass with apparently few combustion inputs (Figure 12B). Five-day back trajectories for much of this relatively well-aged air suggests that it had been over water for this time, with some flows extending to the east, towards the North America continent. The calculated $\Delta CH_4/\Delta CO$ for this air mass is 1.29, and is consistent with urban emission ratios (Table 2). The slope for the relationship between CH_4 and C_2H_6 is unusually high as compared to others seen during the mission (0.14 ppbv/pptv; Table 2) and the correlation between the two gases, as well as that between CH_4 and other hydrocarbons, is unusually low, indicating a well aged air mass that has lost these shorter-lived gases.

Flying in the vicinity of Kona, Hawaii, the DC-8 aircraft noted extensive pollution layers with variable trace gas signatures on flight 19 (6 April). Within the boundary layer, elevated CH_4 and CO are well correlated and appear to have largely urban/industrial sources; correlation is poor with CH_3Cl, which is relatively low (Table 2). Trajectories suggest that this low level air had arrived in the region from the west coast of the U.S. after some days over the ocean. Relatively low CH_3Cl in air from North America is consistent with data reported in Blake et al. (2001) from the tropical Pacific. Air at higher altitudes has trajectories from Indonesia and the western Pacific, extending back as far as India. The CH_4/CO slope in this air mass is roughly half of that in the boundary layer, likely a reflection both of the more southern origin of the air as well as some mixed combustion inputs, as seen in other air masses with these types of trajectories. Upper altitude air appears to be well aged, with an average C_2H_2/CO ratio of 1.34

pptv/ppbv and a C_3H_8/C_2H_6 ratio of 0.07. Values at low altitude were 1.98 and 0.16 respectively, indicating more recent hydrocarbon inputs.

Although emission ratios for CH_4 in specific plumes vary significantly, as shown in Table 2, 5 day back-trajectories suggest that much of this variability is a result of the two dominant air flow patterns at this time (Liu et al., this issue). Frontal lifting ahead of southeastward-moving cold fronts appears to be a major transport pathway moving outflows of Chinese pollution to the Pacific basin. While this air varies in trace gas characteristics depending upon its previous transport history, it commonly has relatively low combustion inputs as indicated by CH_3Cl mixing ratios. It also has somewhat higher $\Delta CH_4/\Delta CO$, $\Delta CH_4/\Delta C_2H_2$, and $\Delta CO/\Delta CO_2$ ratios, and higher or negative $\Delta CH_4/\Delta CH_3Cl$ ratios (Table 2). The other major transport pathway moving continental air into the Pacific basin at this time is characterized by deep convection over the southeast Asian region in conjunction with northeastward transport (Liu et al., this issue). These trajectories tend to carry air masses with enhanced CH_3Cl mixing ratios reflecting the additional inputs of biomass burning occurring in these regions and have generally lower $\Delta CH_4/\Delta CO$ ratios, likely the result of burning inputs of CO. The relationship between CH_4 and C_2H_6 displays relatively little variability between plumes and/or transport pathways (Table 2), suggesting that emission ratios from the dominant sources of fossil fuel usage and biomass burning at this time are relatively constant. Similarity in source emission ratios may in part account for the very high correlation between the two gases observed throughout the region.

5. Changes in CH_4 with Time: Comparison with PEM - West B

Part of the rationale behind the TRACE-P mission was to compare measurements over this region with those made 7 years earlier during PEM - West B (PWB) and to assess any basin-wide changes as industrialization has proceeded on the Asian continent (Jacobs et al., this issue). Because a major objective of both the TRACE-P and PWB missions was to sample and characterize polluted continental outflow to the Pacific, we expect trace gas mixing ratios to be elevated well above clean background levels. Because this objective was common to both missions, they should share a similar sampling bias and comparisons between missions should be possible. As shown in Plate 2, it is clear that significantly different CH_4 mixing ratios were sampled during the two missions. Despite the overall change in concentrations and sparcer geographic coverage however, latitudinal and longitudinal trends similar to those discussed earlier are apparent in Plate 2 for PWB.

5.1 Trends with Latitude

In the Western Pacific below 2 km, TRACE-P mixing ratios average 21 ppbv above CMDL background latitudinal means; during PWB this difference was 26 ppbv. As discussed in Section 4.1, enhancement over background levels is minimal south of 15ºN during TRACE-P. North of 15ºN, enhancements were relatively constant and ranged between 27 and 38 ppbv (Figure 4A). This pattern was somewhat different for PWB, when elevated mixing ratios were sharply higher between 15 and 25ºN, fell somewhat, then increased more gradually with increasing latitude north. Maximum enhancement over background levels was 57 ppbv between 20 and 25ºN. Rather than the broad region of higher concentrations seen during TRACE-P, elevated CH_4 levels were focused in a more restricted area. The average enhancement over CMDL background levels north of 15ºN is similar however between the missions; 31 ppbv

during TRACE-P and 32 ppbv during PWB. Between 5 and 15ºN, little enhancement of CH_4 over CMDL levels is seen for TRACE-P (Figure 4A). During PWB at these latitudes, enhancements were larger and averaged 14 ppbv, resulting in the greater enhancements observed overall for these longitudes.

At Central/Eastern longitudes, average differences between mission and CMDL latitudinal means are 5 and 16 ppbv for TRACE-P and PWB respectively, suggesting that enhancement over background during PWB may have somewhat greater than during TRACE-P. For PWB however, this average difference is based on only 2 latitudinal classes where mission data and the Pacific CMDL site locations (5º latitude means) overlap. However, as Figure 16B suggests, we can linearly extrapolate with only nominal errors between the CMDL 5º latitude means for latitudes with PWB data but without CMDL sites (35-40ºN, 40-45ºN, and 50-55ºN). Using these extrapolations, the average PWB enhancement over Central/Eastern longitudes was 23 ppbv. Elevations over CMDL values were modest north of 40ºN (2 - 6 ppbv), but between 35-40ºN are sharply higher, 78 ppbv. During TRACE-P, enhanced levels decrease with increasing latitude north between 15 and 35ºN, from 13 to -3 ppbv, and as for West longitudes, lack sharp differences between latitudes.

Figure 13 compares latitudinal trends in CH_4 for the two missions in both the Western Pacific and Central/Eastern Pacific. Comparisons between missions are best for the Western Pacific where data for both missions was collected more intensely and there is greater temporal and spatial overlap. On average in the near-surface at these longitudes, CH_4 mixing ratios during TRACE-P are 27 ppbv greater than those of PWB, ranging from 11 to 47 ppbv. The smallest difference is observed between the latitudes of 20 and 25ºN where CH_4 inputs are high during

PWB and the greatest enhancement over CMDL clean air levels is seen. Average near-surface differences between missions for other hydrocarbons are negative, with PWB mixing ratios higher than those for TRACE-P; by 209 pptv for C_2H_6, 138 pptv for C_2H_2, and 222 pptv for C_3H_8. Although the several week offset in timing between the two missions may contribute to these differences, we would expect that it would be opposite in sign, with PWB concentrations less than TRACE-P.

Latitudinal trends for C_2H_6 and C_2Cl_4 in the West Pacific for the two missions are shown in Figure 14. Near-surface ethane levels at latitudes south of 20°N appear to be quite similar between missions while greater mixing ratios between 20 and 25°N and north of 35°N are observed during PWB (Figure 14A). Mixing ratios of C_2Cl_4 are also strikingly higher in the near-surface of PWB, by an average of 10.7 pptv, while those for CH_3Cl are almost identical, differing by an average of only 2 pptv. These differences may suggest that PWB observed greater anthropogenic inputs in this region than during TRACE-P and comparable combustion inputs (Figure 14A). However, significant differences in the usage of C_2Cl_4 occurred between the two missions, accounting for at least part of this change (McCulloch, et al., 1999; U.S. EPA, 1994; Schettler et al., 1999). Differences in trace gases are also likely to reflect any sampling bias between the missions. Although many of the objectives of the expeditions were similar, they were not identical and the execution of objectives no doubt varied.

In the mid-troposphere, between 2 and 6 km (Figure 14B), average PWB NMHC and C_2Cl_4 levels are also greater than those of TRACE-P, although average differences are smaller than those below 2 km (182 pptv C_2H_6, 47 pptv C_2H_2, 115 pptv C_3H_8, and 6.6 pptv C_2Cl_4). Latitudinal CH_4 means are on average 29 ppbv higher for TRACE-P, similar to the difference

seen in near-surface values, and CH_3Cl is again comparable. Above 6 km (Fig. 14C), the trend of decreasing differences continues and average NMHC mixing ratios from TRACE-P are greater than those of PWB, although differences themselves are relatively small (81 pptv C_2H_6, 40 pptv C_2H_2, 32 pptv C_3H_8). TRACE-P mixing ratios of C_2Cl_4 were still somewhat lower (2.8 pptv), while CH_4 differences were greater, 39 ppbv. As seen in Figure 14, average C_2H_6 and C_2Cl_4 mixing ratios within the Western Pacific are highly correlated for both missions.

5.2 Trends with Altitude

As shown in Figure 15, average altitude profiles during PWB for CH_4 and a variety of other hydrocarbons appear to be quite similar to those seen in TRACE-P (Figure 8) and the high correlation between CH_4 and these gases was also present during the mission. As for TRACE-P, coefficients of determination are high for the relationships between these trace gases ($\Delta CH_4/\Delta CO$=0.74, r^2=0.79; $\Delta CH_4/\Delta C_2H_6$=0.046 ppbv/pptv, r^2=0.91; $\Delta CH_4/\Delta C_2Cl_4$,=4.56 ppbv/pptv, r^2=0.85). The relationship between CH_4 and C_2H_6 is identical to that of TRACE-P, but the PWB regression slopes for CH_4 and CO and for CH_4 and C_2Cl_4 differ, consistent with the hypothesis that greater urban/industrial inputs may have been sampled during PWB. The regression slope of CH_4 with CO is steeper in PWB (0.74 vs. 0.58 for TRACE-P) and that with C_2Cl_4 is shallower (4.56 vs. 7.37 ppbv/pptv for TRACE-P), reflecting higher C_2Cl_4 inputs and the relatively CH_4-enriched emissions from urban sources as compared to biomass or biofuel burning.

5.3 Regional Comparisons

Plates 1 and 2 highlight the significant difference in overall CH_4 levels observed across the Pacific Basin over a 7 year time interval. These differences however, include contributions

from any seasonal disparities between the mission and changes in the global background levels, as well as any possible meteorological variability and source changes. In order to examine any air quality changes due to industrialization and land use change, we must account for these other contributions.

Although TRACE-P and PWB were conducted at roughly the same time of year, they were offset by several weeks, a concern for a trace gas such as CH_4 with a significant seasonal cycle. Monthly averages based on CMDL Pacific background air samples (Figure 16A) suggest that this source of variability is relatively small for CH_4, but that the increase over the 7 years between the missions is large. Although there can be significant longitudinal variability in CH_4, as shown above in Section 4.3, longitudinal variability in background levels for a long-lived trace gas such as CH_4 is much smaller than that due to differences in the latitudinal distribution of sources (Dlugokencky et al., 1994). To derive an estimate of the background change, we calculate seasonally-weighted average CH_4 mixing ratios for the CMDL Pacific sites for the duration of the missions from monthly averages. To reduce site-specific variability, these averages were grouped into 5° latitude classes. As shown in Figure 16B, these mission averages suggest a relatively constant latitudinal difference between CMDL clean air values between the PWB and TRACE-P time periods over the domain of most interest between 10°N and 40°N, with perhaps a somewhat smaller difference above 30°N. Latitudinal variability in background differences may in part be due to differential growth in source types. Between 50°S and 30°N, differences in CMDL background levels range from 12 to 55 ppbv and average 41 ± 7 (1σ). Similar calculations for background sites outside of the Pacific basin yield comparable differences and average 31 ± 14 ppbv (data not shown; 90°S - 30°N). Using all the CMDL

background sites, we derive a global background difference of 38 ± 6 ppbv for latitudes south of 30°N between the two missions. Above 30°N, differences average 25 ± 10 ppbv in the Pacific and 29 ± 14 ppbv for non-Pacific sites, yielding a global average of 27 ± 12 ppbv. Although lower latitude sites in the Pacific basin tend to have slightly higher differences between missions, suggesting perhaps that sources may have increased there more than in other regions, these differences are not statistically significant.

Assuming that the meteorological setting of the two missions is roughly similar, as indicated by Fuelberg et al. (this issue), and that transport of continental outflows were comparably sampled, calculations based on the observed changes in background mixing ratios suggest that the average changes in CH_4 seen between missions, on the order of 30 - 40 ppbv (Section 5.1), are likely to be largely a result of an increasing background rather than an additional change in emissions due to changing land use and/or industrialization. Methane is a long-lived trace gas so that upper altitude concentrations should reflect those at surface-level since rates of mixing are rapid relative to those of photochemical loss. This assumption seems reasonable since differences between missions at 2 - 6 km and above 6 km are similar to those in the well mixed boundary layer. The high correlation observed for both missions between CH_4 and other hydrocarbons such as C_2H_6, not thought to have significant long-term background trends because of their shorter atmospheric lifetimes, may however, provide an additional way to examine the change in CH_4 at all altitudes between the two missions.

In Figure 17, we show the correlation between differences in CH_4 and C_2H_6 between PWB and TRACE-P for highly averaged spatial data. The data used to calculate differences are 1 km altitude means for 6 large geographic regions, the broad latitude and longitude classes

discussed previously (south of 20°N, 20 - 40°N, north of 40°N and either east or west of 160°E). As shown in Figure 17 and discussed above, variability in CH_4 and C_2H_6 between PWB and TRACE-P are highly correlated. Based on this relationship and the assumption that there is little long-term change in C_2H_6, the y-intercept yields an estimate of the change in CH_4 between the missions. For all of the data shown in Figure 17, this value is 38 ppbv (r^2=0.79, n=53), and the $\Delta CH_4/\Delta C_2H_6$=0.041 ppbv/pptv, in agreement with the relationship between these gases observed in specific plumes and in spatial averages. This calculation is complicated however, by the presence of a seasonal cycle in C_2H_6 and the seasonal offset between the two missions. For the relatively long-lived CH_4, this is a minor effect (Figure 16A), in part because seasonal variability is only a fraction of a large background. For the shorter-lived hydrocarbons, however, it is a more significant concern. Seasonal variability in C_2H_6 is greatest in the high northern latitudes (Rudolph, 1995), a function both of greater seasonal changes in the atmospheric OH sink in the north and the latitudinal distribution of sources. It should also be greatest at lower altitudes, where variability is higher. Here, we can partially take the seasonal cycle and the several week offset between the missions into account by only using data from the <20°N and 20 - 40°N latitude classes. Restricting the data in Figure 17 in this way demonstrates that much of the variability seen for negative C_2H_6 change between missions (PWB higher than TRACE-P) occurs north of 40°N. The largest of these negative values are observed at altitudes below 3 km. The correlation between changes in CH_4 and C_2H_6 is improved by eliminating the higher latitude data, yielding a coefficient of determination (r^2) of 0.92, but results in little alteration in the calculated CH_4 change "offset" which remains 38 ppbv, because the relationship for all of the data is driven largely by these lower latitude values. The $\Delta CH_4/\Delta C_2H_6$=0.052 ppbv/pptv, somewhat higher

than for the data as a whole (0.041), but is still within observed values.

Dispersion along the regression line in Figure 17 is an indirect measure of spatial variability between the missions, since we would expect points to form a cluster at 0 change for C_2H_6 and roughly 38 ppbv for CH_4 if geographic regions were perfectly paired. Note that for C_2H_6, positive and negative mission differences are roughly equal and average a non-significant -41 ± 296 pptv, indicating that there was little sampling bias, such as a disproportionate sampling of plumes, between the missions. These calculations of course, shed little light on any effects of sampling bias on the regional representativeness of the observations.

Similar calculations for changes between missions in CH_4 and C_2H_2 yield a "change offset" of 34 ppbv (r^2=0.73, n=53, $\Delta CH_4/\Delta C_2H_2$=0.074 ppbv/pptv for all of the data, and 36 ppbv, r^2=0.81, $\Delta CH_4/\Delta C_2H_2$=0.089 ppbv/pptv, n=37, for data south of 40°N). For CH_4 and C_3H_8, this value is 41 ppbv for all data (r^2=0.66, n=53, $\Delta CH_4/\Delta C_3H_8$=0.060 ppbv/pptv) and 41 ppbv (r^2=0.84, n=37, $\Delta CH_4/\Delta C_3H_8$=0.097 ppbv/pptv) for data south of 40°N. The small decrease in correlation coefficient from C_2H_6, to C_2H_2, and C_3H_8 is likely a reflection of the increasing difference in atmospheric lifetime between CH_4 and the hydrocarbons as the shorter-lived hydrocarbons begin photochemical loss within a few days and source emission ratios are altered from their original values. Seasonal cycles also differ somewhat between the hydrocarbons as the shorter-lived gases decrease more rapidly in spring (Blake et al., this issue).

Although we expect that the close correlation between CH_4 and the other hydrocarbons has a functional basis since they are linked through many of their sources, we can undertake similar calculations for the well-correlated changes between missions of C_2Cl_4, using C_2H_6 as a baseline for an anthropogenic source with little long-term change. In this case, C_2Cl_4 is lower

during TRACE-P than PWB, yielding a change offset of -4.9 pptv for the data as a whole (r^2=0.74, n=53, $\Delta C_2Cl_4/\Delta C_2H_2$=0.010). Excluding the northernmost latitude class in this case results in a decrease in the explained variability (C_2Cl_4 change offset=-6.2 pptv; r^2=0.43, n=37, $\Delta C_2Cl_4/\Delta C_2H_2$=0.121). Explanation for this difference is likely to lie in the northerly distribution of C_2Cl_4 sources.

Correlations between changes between missions in CH_4 and other correlated trace gases such as CO can also be calculated. For CO, the relationship between the two is not as strong, in part because major sources such as combustion and fossil fuel use vary in their CH_4/CO ratios. Differences between missions yield a "change offset" for CH_4 of 29 ppbv (r^2=0.55, n=53, $\Delta CH_4/\Delta CO$=0.45), lower than calculated with the hydrocarbons, and suggest that either the relative mix of sources may be different between the two missions, as discussed in Section 5.3, or that the assumption of little to no long-term change in CO is invalid. Restricting the data to latitudes south of 40°N improves the correlation between CH_4 and CO (CH_4 offset=31 ppbv, r^2=0.70, n=39, $\Delta CH_4/\Delta CO$=0.58), probably due to latitudinal differences in the CO seasonal cycle as for C_2H_6. Calculations using changes in C_2H_2/CO ratios and CH_4 yield values in agreement with those using hydrocarbons (y-intercept=36 ppbv, r^2=0.81, n=53, $\Delta CH_4/\Delta C_2H_2/CO$=18.8), probably largely due to the correlation with C_2H_2. Restricting the data to latitudes south of 40°N makes relatively little change (CH_4 offset=35 ppbv, r^2=0.84, n=39, $\Delta CH_4/\Delta C_2H_2/CO$=19.3).

Agreement between the various hydrocarbons for estimating a basin-wide mission difference in CH_4 is excellent and their consistency with the calculated background change derived from CMDL surface data both confirms the assumption that there is little long-term

change in the NMHCs as well as the conclusion that changes in Asian industrialization and land use over the last 7 years are not reflected in obvious additional changes in levels of CH_4 throughout the air column. Given the relatively long atmospheric lifetime of CH_4 this may not be an unexpected finding since changes in emissions are integrated into background levels and the response time of atmospheric mixing ratios to changes in emissions is fairly rapid (see for example, Tans, 1997).

Summary

The high-resolution, high-precision CH_4 data set collected during TRACE-P over the Asian spring highlights the importance of continental outflow to the North Pacific Basin at this time. Trace gas ratios ($\Delta CH_4/\Delta CO$) and source-specific tracers such as C_2Cl_4 for urban/industrial sources, and CH_3Cl for combustion, indicate that these outflows are complex mixtures of trace gases from a variety of sources that are rapidly carried into the basin by the strong westerly transport characteristic of this time of year (Fuelberg et al., this issue). Five-day trajectories calculated for elevated trace gases in plume layers suggest that sources as far upwind as Africa, India, Southeast Asia, and Siberia make contributions to the pollution observed during the mission. Trajectories from the south and west (Africa, India, Southeast Asia) tend to carry trace gas signatures indicating higher inputs from combustion sources than those from the northwest (Siberia, northern China). Overall, the high correlations between spatially averaged CH_4 mixing ratios and those of C_2H_6 and other hydrocarbons, as well as C_2Cl_4, indicate that urban/industrial sources dominate regional inputs. Comparisons between measurements made during TRACE-P and those of PEM - West B, flown during roughly the same time of year and under a similar

meteorological setting 7 years earlier, suggest that although the TRACE-P CH_4 observations are significantly higher, the changes largely parallel the changes seen in clean, background air over this time interval. Although clearly significant changes in population, land use, and industrialization have occurred between the two missions, these comparisons would imply that any regional emission changes are difficult to isolate from those upwind and are not reflected in basin-wide changes in CH_4 levels over and above the changes already included in the baseline rise of this long-lived trace gas.

Acknowledgments

This work was made possible by support from the NASA GTE program and we wish to thank the GTE staff, lead by Dr. Vickie Connors, for their help. Excellent logistical support on this complex expedition was provided by the pilots, missions managers, and crew of the Wallops P-3B and the Dryden DC-8 aircraft. We greatly appreciate use of data on background levels of CH_4, provided courtesy of the Climate Monitoring and Diagnostic Laboratory (CMDL). We also appreciate the thoughtful comments of Nicola Blake on an earlier manuscript version.

References Cited

Andreae, M.O., E. Atlas, G.W. Harris, G. Helas, A. de Kock, R. Koppmann, W. Maenhaut, S. Manø, W.H. Pollock, J. Rudolph, D. Scharffe, G. Schebeske, and M. Welling, Methyl halide emissions from savanna fires in southern Africa, *J. Geophys. Res.*, *101*, 23,603-23,613, 1996.

Bartlett, K.B., G.W. Sachse, J.E. Collins Jr, and R.C. Harriss, Methane in the tropical South Atlantic: Sources and distribution during the late dry season, *J. Geophys. Res.*, *101*, 24,139-24,150, 1996.

Bey, I., D.J. Jacob, J.A. Logan, and R.M. Yantosca, Asian chemical outflow to the Pacific in spring: Origins, pathways, and budgets, *J. Geophys. Res.*, *106*, 23,097-23,113, 2001.

Bey, I., et al., this issue ("Using chemical forecasts for the planning of an aircraft missions: Success and weakness")

Blake, D.R., and F.S. Rowland, Continuing world-wide increase in tropospheric methane, 1978 - 1987, *Science*, *239*, 1129-1131, 1988.

Blake, N.J., D.R. Blake, B.C. Sive, T.-Y. Chen, F.S. Rowland, J.E. Collins Jr, G.W. Sachse, and B.E. Anderson, Biomass burning emissions and vertical distribution of atmospheric methyl halides and other reduced carbon gases in the South Atlantic region, *J. Geophys. Res.*, *101*, 25,151-24,164, 1996.

Blake, N.J., D.R. Blake, I.J. Simpson, J.P. Lopez, N.A.C. Johnson, A.L. Swanson, A.S. Katzenstein, S. Meinardi, B.C. Sive, J.J. Colman, E. Atlas, F. Flocke, S.A. Vay, M.A. Avery, and F.S. Rowland, Large-scale latitudinal and vertical distribution of NMHCs and selected halocarbons in the troposphere over the Pacific Ocean during the March - April 1999 Pacific Exploratory Mission (PEM - Tropics B), *J. Geophys. Res.*, *106*, 32,627-32,644, 2001.

Blake et al., this issue (NMHC paper)

Blake, N.J., D.R. Blake, T.-Y. Chen, J.E. Collins Jr, G.W. Sachse, B.E. Anderson, and F.S. Rowland, Distribution and seasonality of selected hydrocarbons and halocarbons over the western Pacific basin during PEM - West A and PEM - West B, *J. Geophys. Res.*, *102*, 28,315-28,331, 1997.

Bräunlich, M., O. Aballain, T. Marik, P. Jöckel, C.A.M. Brenninkmeijer, J. Chappellaz, J.-M. Barnola, R. Mulvaney, and W.T. Sturges, Changes in the global atmospheric methane budget over the last decades inferred from ^{13}C and D isotopic analysis of Antarctic firn air, *J. Geophys. Res.*, *106*, 20,465-20,481, 2001.

Brocard, D., J.-P. Lacaux, and H. Eva, Domestic biomass combustion and associated atmospheric emissions in West Africa, *Global Biogeochem. Cycles*, *12*, 127-139, 1998.

Browell, E.V., et al., this issue (air mass characterization)

Cooke, W.F., B. Koffi, and J.-M. Grégoire, Seasonality of vegetation fires in Africa from remote sensing data and application to a global chemistry model, *J. Geophys. Res.*, *101*, 21,051-21,065, 1996.

Ferek, R.J., J.S. Reid, P.V. Hobbs, D.R. Blake, and C. Liousse, Emission factors of

hydrocarbons, halocarbons, trace gases and particles from biomass burning in Brazil, *J. Geophys. Res.*, *103*, 32,107-32,118, 1998.

Francey, R.J., M.R. Manning, C.E. Allison, S.A. Coram, D.M. Etheridge, R.L. Langenfelds, D.C. Lowe, and L.P. Steele, A history of $\delta^{13}C$ in atmospheric CH_4 from the Cape Grim air archive and Antarctic firn air, *J. Geophys. Res.*, *104*, 23,631-23,643, 1999.

Dlugokencky, E.J., L.P. Steele, P.M. Lang, and K.A. Masarie, The growth rate and distribution of atmospheric methane, *J. Geophys. Res.*, *99*, 17,021-17,043, 1994.

Dlugokencky, E.J., K.A. Masarie, P.M. Lang, and P.P. Tans, Continuing decline in the growth rate of the atmospheric methane burden, *Nature*, *393*, 447-450, 1998.

Ehhalt, D.H., F. Rohrer, A.B. Knaus, M.J. Prather, D.R. Blake, and F.S. Rowland, On the significance of regional trace gas distributions as dervived from aircraft campaigns in PEM - West A and B, *J. Geophys. Res.*, *102*, 28,333-28,351, 1997.

Fuelberg, H.E., C.M. Kiley, J.R. Hannan, D.J. Westberg, M.A. Avery, and R.E. Newell, Atmospheric transport during the **Tr**ansport and **C**hemical **E**volution over the **P**acific (TRACE-P) experiment, *J. Geophys. Res.*, this issue.

Gupta, M., S. Tyler, and R. Cicerone, Modeling atmospheric $\delta^{13}CH_4$ and the causes of recent changes in atmospheric CH_4 amounts, *J. Geophys. Res.*, *101*, 22,923-22,932, 1996.

Hao, W.M. and M.-H. Liu, Spatial and temporal distribution of tropical biomass burning, *Global Biogeochem. Cycles*, *8*, 495-503, 1994.

Heald, C.L., D.J. Jacob, P.I. Palmer, et al., Biomass burning emission inventory with daily resolution: Application to aircraft observations of Asian outflow, this issue.

Hoell, J.M., D.D. Davis, S.C. Liu, R.E. Newell, H. Akimoto, R.J. McNeal, and R.J. Bendura, The Pacific Exploratory Mission - West Phase B: February - March 1994, *J. Geophys. Res.*, *102*, 28,223-28,239, 1997.

Jacob, D.J. et al., this issue (overview paper on experimental design)

Khalil, M.A.K., R.A. Rasmussen, M.J. Shearer, R.W. Dalluge, L. Ren, and C.-L. Duan, Factors affecting methane emissions from rice fields, *J. Geophys. Res.*, *103*, 25,219-25,231, 1998.

Kleb, M. et al., this issue ("The TRACE-P experiment: Implementation details and data sets")

Lelieveld, J., P.J. Crutzen, V. Ramanathan, M.O. Andreae, C.A.M. Brenninkmeijer, T. Campos, G.R. Cass, R.R. Dickerson, H. Fischer, J.A. de Gouw, A. Hansel, A. Jefferson, D. Kley,

A.T.J. de Laat, S. Lal, M.G. Lawrence, J.M. Lobert, O.L. Mayol-Bracero, A.P. Mitra, T. Novakov, S.J. Oltmans, K.A. Prather, T. Reiner, H. Rodhe, H.A. Scheeren, D. Sikka, and J. Williams, The Indian Ocean Experiment: Widespread pollution from South and Southeast Asia, *Science*, *291*, 1031-1036, 2001.

Liu, H., D.J. Jacob, I. Bey, R.M. Yantosca, B.N. Duncan, and G.W. Sachse, Transport pathways for Asian combustion outflow over the Pacific: Interannual and seasonal variations, *J. Geophys. Res.*, this issue.

Lobert, J.M., D.H. Scharffe, W.-M. Hao, T.A. Kuhlbusch, R. Seuwen, P. Warneck, and P.J. Crutzen, Experimental evaluation of biomass burning emissions: Nitrogen and carbon containing compounds, in *Global Biomass Burning - Atmospheric, Climatic, and Biospheric Implications*, edited by J.S. Levine, MIT Press, Cambridge, MA, 1991.

Matthews, E., I. Fung, and J. Lerner, Methane emission from rice cultivation: Geographic and seasonal distribution of cultivated areas and emissions, *Global Biogeochem. Cycles*, *5*, 3-24, 1991.

McCulloch, A., M.L. Aucott, T.E. Graedel, G. Kleiman, P.M. Midgley, Y.-F. Li, Industrial emissions of trichloroethene, tetrachloroethene, and dichloromethane: Reactive Chlorine Emissions Inventory, *J. Geophys. Res.*, *104*, 8417-8428, 1999.

McKeen, S.A., S.C. Liu, E.-Y. Hsie, X. Lin, J.D. Bradshaw, S. Smyth, G.L.Gregory, and D.R. Blake, Hydrocarbon ratios during PEM - West A: A model perspective, *J. Geophys. Res.*, *101*, 2087-2109, 1996.

Merrill, J.T., R.E. Newell, and A.S. Bachmeier, A meteorological overview for the Pacific Exploratory Mission - West Phase B, *J. Geophys. Res.*, *102*, 28,241-28,253, 1997.

Parrish, D.D., C.J. Hahn, E.J. Williams, R.B. Norton, F.C. Fehsenfeld, H.B. Singh, J.D. Shetter, B.W. Gandrud, and B.A. Ridley, Indications of photochemical histories of Pacific air masses from measurements of atmospheric trace species at Point Arena, California, *J. Geophys. Res.*, *97*, 15,883-15,902, 1992.

Prinn, R.G., R.F. Weiss, B.R. Miller, J. Huang, F.N. Alyea, D.M. Cunnold, P.J. Fraser, D.E. Hartley, and P.G. Simmons, Atmospheric trends and lifetimes of CH_3CCl_3 and global OH concentrations, *Science*, *269*, 187-192, 1995.

Randriambelo, T., J.-L. Baray, and S. Baldy, Effect of biomass burning, convective venting, and transport on tropospheric ozone over the Indian Ocean: Reunion Island field observations, *J. Geophys. Res.*, *105*, 11,813-11,832, 2000.

Rasmussen, R.A., L.E. Rasmussen, M.A.K. Khalil, and R.W. Dalluge, Concentration distribution

of methyl chloride in the atmosphere, *J. Geophys. Res.*, *85*, 7350-7356, 1980.

Rudolph, J., The tropospheric distribution and budget of ethane, *J. Geophys. Res.*, *100*, 11,369-11,381, 1995.

Sachse, G.W., G.F. Hill, L.O. Wade, and M.G. Perry, Fast-response, high-precision carbon monoxide sensor using a tunable diode laser absorption technique, *J. Geophys. Res.*, *92*, 2071-2081, 1987.

Sachse, G.W., J.E. Collins, G.F. Hill, L.O. Wade, L.G. Burney, and J.A. Ritter, Airborne tunable diode laser sensor for high precision concentration and flux measurements of carbon monoxide and methane, *Proc. SPIE Int. Opt. Eng.*, *1433*, 145-156, 1991.

Schettler, T., G. Solomon, M. Valenti, and A. Huddle, *Generations at Risk: Reproductive Health and the Environment*, The MIT Press, Cambridge, Massachusetts, 417 p., 1999.

Scholes, R.J., D.E. Ward, and C.O. Justice, Emission of trace gases and aerosol particles due to vegetation burning in southern hemisphere Africa, *J. Geophys. Res.*, *101*, 23,677-23,682, 1996.

Schultz, M.G. et al., this issue (forecasts of CO w/ a GCM)

Streets, D.G., K. Jiang, X. Hu, J.E. Sinton, X.-Q., Zhang, D. Xu, M.Z. Jacobson, and J.E. Hansen, Recent reductions in China's greenhouse gas emissions, *Science*, *294*, 1835-1837, 2001.

.

Streets, D.G. et al., An inventory of gaseous and primary aerosol emissions in Asia in the year 2000, this issue.

Talbot, R.W., J.E. Dibb, B.L. Lefer, J.D. Bradshaw, S.T. Sandholm, D.R. Blake, N.J. Blake, G.W. Sachse, J.E. Collins, Jr., B.G. Heikes, J.T. Merrill, G.L. Gregory, B.E. Anderson, H.B. Singh, D.C. Thornton, A.R. Bandy, and R.F. Pueschel, Chemical characteristics of continental outflow from Asia to the troposphere over the western Pacific Ocean during February - March 1994: Results from PEM - West B, *J. Geophys. Res.*, *102*, 28,255-28,274, 1997.

Tans, P.P., A note on isotopic ratios and the global atmospheric methane budget, *Global Biogeochem. Cycles*, *11*, 77-81, 1997.

U. S. EPA, Chemicals in the Environment: Perchloroethylene (CAS No. 127-18-4), Office of Pollution Prevention and Toxics Chemical Fact Sheet, Environmental Protection Agency, 1994.

Wang, C. J.-L., D.R. Blake, and R.S. Rowland, Seasonal variations in the atmospheric distribution of a reactive chlorine compound, tetrachloroethene (CCl_2=CCl_2), *Geophys. Res. Lett.*, *22*, 1097-1100, 1995.

Yao, H., Y.-H. Zhuang, and Z.L. Chen, Estimation of methane emissions from rice paddies in mainland China, *Global Biogeochem. Cycles*, *10*, 641-649, 1996.

Figure and Plate Captions:

Figure 1: A) Correlation between DACOM and UCI CH_4 measurements for "simultaneous" 1 min merged data. Solid squares denote data with differences > 2 σ.
B) Frequency distribution of differences between DACOM and UCI CH_4 data.

Figure 2: All TRACE-P data above 6 km. Open squares are observations classified as having a significant stratospheric input.

Figure 3: Frequency distribution for all TRACE-P data by altitude.

Figure 4: A) Latitudinally averaged CH_4 mixing ratios in the Western Pacific (west of 160°E), 5° latitude classes. Averaged CMDL values are for Pacific basin sites only and are means of 5° latitude.
B) As for Figure 4A, Central/Eastern Pacific (east of 160°E).

Figure 5: Longitudinally averaged CH_4 mixing ratios by latitude class. Dashed line at 160°E marks the break between the Western Pacific longitude class and the Central/Eastern Pacific class.
A) North of 40°N; B) 20°N - 40°N; C) South of 20°N.

Figure 6: As for Figure 5B, averages with longitude within 20°N - 40°N. A) CO; B) C_2H_6; C) C_2H_2; D) C_2Cl_4; and E) CH_3Cl.

Figure 7: Average altitude profiles by latitude class. For the Western Pacific (west of 160°E): A) CH_4; B) C_2H_6; C) C_2Cl_4; D) CH_3Cl; E) CO. For the Central/Eastern Pacific (east of 160°E): F) CH_4; G) C_2H_6; H) C_2Cl_4; I) CH_3Cl; J) CO.

Figure 8: Average altitude profiles for CH_4 and selected hydrocarbons, 20°N - 40°N; 20° longitude classes. A) 100-120°E; B) 120-140°E; C) 140-160°E; and D) 160-180°E.

Figure 9: Shanghai plume, DC-8 Flight 13. Triangles: CH_4; Crosses: CH_3Cl.

Figure 10: Methane mixing ratios during DC-8, Flight 10. For CH_4 - Open circles: above ~ 5 km; Solid circles: below ~ 5 km. For CH_3Cl - Open triangles: above ~ 5 km; Solid triangles: below ~ 5 km.

Figure 11: Methane mixing ratios for air masses sampled during P-3B Flight 9. A) CH_4 and CH_3Cl; B) CH_4 and C_2Cl_4. Solid squares: Air with tropical trajectories; Crosses: Near-surface plume; Open squares: Air with southwest trajectories.

Figure 12: Methane mixing ratios for air masses sampled during P-3B Flight 6. A) CH_4 and CO; B) CH_4 and CH_3Cl. Open squares: Tropical oceanic trajectories; Open triangles:

plume at 3 km; Solid squares: near-surface pollution.

Figure 13: Latitudinal trends by longitude class and altitude for PEM - West B and TRACE-P. A) 0 - 2 km; B) 2 - 6 km; and C) > 6 km.

Figure 14: Latitudinal trends with altitude in the West Pacific (west of 160°E) for ethane (C_2H_6) and perchloroethene (C_2Cl_4). A) 0 - 2 km; B) 2 - 6 km; and C) > 6 km.

Figure 15: PEM - West B average altitude profiles for CH_4 and selected hydrocarbons, 20°N - 40°N; 20° longitude classes; as for Figure 8 for TRACE-P. A) 100-120°E; B) 120-140°E; C) 140-160°E; and D) 160-180°E.

Figure 16: A) Monthly average CH_4 mixing ratios for Pacific Basin CMDL sites during the PEM - West B and TRACE-P missions, by latitude. Elevated values at 36.7°N are for the Tae-ahn Peninsula, Korea, known to have high CH_4 levels.
B) As for A, but averaged for the duration of the missions and grouped into 5° latitude classes.

Figure 17: Differences in spatially averaged CH_4 and C_2H_6 mixing ratios between PEM - West B and TRACE-P. Data are 1 km altitude averages for three latitude classes (north of 40°N, 20°N - 40°N, south of 20°N) and two longitude classes (west of 160°E and east of 160°E). Open squares: North of 40°N; solid squares: 20°N - 40°N and south of 20°N.

Plate 1: Regional distribution of CH_4 during the TRACE-P expedition; 0 - 2 km, 2 - 6 km, and above 6 km. Data were grouped into 2.5° latitude x 2.5° longitude areas then averaged. Number of observations within areas vary.

Plate 2: Regional distribution of CH_4 during PEM - West B, as for Plate 1.

Table 1: TRACE-P Regional Characterization for Selected Trace Gases; average values for broad longitude, latitude, and altitude classes.

Longitude	Latitude	Altitude, km	CO, ppbv	CH_4, ppbv	CO_2, ppmv	C_2Cl_4, pptv	CH_3Cl, pptv	C_2H_6, pptv	C_2H_2, pptv	C_3H_8, pptv	C_2H_2/CO, pptv/ppbv
West (<160°E)	< 20°N	0-2	187	1803	374	7.0	608	1385	579	290	2.4
		2-6	102	1764	372	3.1	566	685	155	63	1.4
		> 6	96	1760	37	2.4	578	610	122	60	1.2
	20°-40°N	0-2	232	1838	377	14.5	592	2111	790	716	3.2
		2-6	156	1793	374	6.5	576	1362	410	294	2.3
		> 6	120	1768	372	3.1	578	798	227	109	1.7
	> 40°N	0-2	202	1844	378	11.3	546	2249	700	779	3.5
		2-6	169	1817	376	9.9	551	1815	520	516	3.0
		> 6	163	1821	376	10.9	541	1900	500	567	3.0
Central/East (> 160°E)	< 20°N	0-2	123	1798	374	5.8	543	1070	187	115	1.5
		2-6	135	1775	373	3.9	578	897	277	90	1.9
		> 6	76	175	371	0.8	546	496	71	21	0.9
	20°-40°N	0-2	137	1798	374	7.2	547	1362	304	274	2.1

		2-6	126	1773	373	4.6	565	1008	248	141	1.8
		> 6	124	1774	373	3.7	574	892	260	109	1.8
	> 40ºN	0-2	134	1824	374	7.7	534	1489	380	453	2.8
		2-6	137	1818	374	10.0	556	1428	412	376	2.6
		> 6	178	1819	374	6.6	612	1426	609	311	3.1

Table 2: Correlations between Selected Trace Gases in Plumes; slopes ($\Delta y/\Delta x$) and coefficients of determination (r^2). Variables are given as y:x. Correlations below the 95% significance level are denoted as NS (not significant). Number of data points used in a regression are given as N for regressions of CH_4 with CO or CO_2 and N_{HC} for regressions with halocarbons and other hydrocarbons. Predominant transport pathways based on 5 day back-trajectories denoted as "**NW**" (generally across China from the northwest, extending back to central Asia or Siberia) or "**SW**" origin (generally across southern China from the southwest, extending back to SE Asia, India, the Middle East, or Africa).

Flight	Air Mass	CH_4:CO, ppbv:ppbv	CH_4:CO_2, ppbv:ppmv	CH_4:C_2H_6, ppbv:pptv	CH_4:C_2H_2, ppbv:pptv	CH_4:C_3H_8, ppbv:pptv	CH_4:C_2Cl_4, ppbv:pptv	CH_4:CH_3Cl, ppbv:pptv	CO:CO_2, ppbv:ppmv	C_2H_6:CO pptv:ppbv
DC-8, #13	Shanghai; N=47, N_{HC}=37; China/**NW** origin	0.22 (0.90)	8.84 (0.57)	0.052 (0.84)	0.021 (0.81)	0.052 (0.73)	1.65 (0.73)	0.16 (0.81)	37.5 (0.71)	5.62 (0.85)
DC-8, #10	near-surface; N=148, N_{HC}=62; **NW** origin	0.39 (0.75)	13.6 (0.86)	0.051 (0.76)	0.123 (0.88)	0.087 (0.34)	7.68 (0.81)	1.20 (0.43)	28.5 (0.91)	7.48 (0.55)
	above ~4 km; N=257, N_{HC}=131; **SW** origin	0.38 (0.48)	8.67 (0.37)	0.048 (0.40)	0.093 (0.42)	0.190 (0.42)	9.32 (0.42)	0.33 (0.41)	22.3 (0.75)	6.61 (0.83)
P-3, #9	tropical; N=102, N_{HC}=33	0.24 (0.48)	NS	0.028 (0.04)	NS	NS	NS	NS	NS	3.94 (0.45)
	Hong Kong outflow; N=267, N_{HC}=117; **SW** origin	0.22 (0.69)	12.8 (0.81)	0.043 (0.82)	0.052 (0.66)	0.148 (0.82)	7.47 (0.62)	0.38 (0.59)	51.9 (0.90)	5.55 (0.89)
	near-surface plume; N=93, N_{HC}=55; **NW** origin	0.45 (0.49)	12.6 (0.94)	0.035 (0.92)	0.083 (0.81)	0.049 (0.89)	7.56 (0.94)	-0.66 (0.69)	14.0 (0.46)	17.4 (0.57)
P-3, #6	plume at 3 km; N=171, N_{HC}=88; **NW** origin	0.33 (0.72)	19.4 (0.41)	0.064 (0.52)	0.086 (0.67)	0.212 (0.21)	10.71 (0.37)	0.436 (0.63)	66.8 (0.73)	3.97 (0.74)
	generally low altitude; N=126, N_{HC}=65; aged marine	1.29 (0.64)	30.2 (0.37)	0.136 (0.40)	0.228 (0.11)	0.481 (0.24)	29.9 (0.47)	-1.07 (0.11)	15.5 (0.26)	5.68 (0.52)

DC-8, #19	near-surface plume; N=248, N_{HC}=142; **NW** origin	0.62 (0.70)	16.46 (0.82)	0.050 (0.70)	0.148 (0.58)	0.126 (0.52)	8.01 (0.80)	NS	20.50 (0.71)	9.53 (0.61)
	above ~ 5 km; N=306, N_{HC}=159; **SW** origin	0.33 (0.73)	12.16 (0.83)	0.048 (0.79)	0.106 (0.62)	0.292 (0.71)	10.58 (0.71)	NS	32.3 (0.91)	7.23 (0.90)
DC-8, #14	Low altitude plume; N=203, N_{HC}=108; **NW** origin	0.71 (0.72)	12.4 (0.72)	0.051 (0.82)	0.132 (0.68)	0.104 (0.75)	6.98 (0.75)	NS	16.2 (0.94)	12.8 (0.76)
	plume at higher altitude; N=350, N_{HC}=192; **SW** origin	0.34 (0.39)	13.8 (0.39)	0.078 (0.67)	0.073 (0.33)	0.210 (0.44)	8.12 (0.50)	0.40 (0.21)	34.9 (0.80)	4.56 (0.65)
DC-8, #12	low altitude plume; N=50, N_{HC}=30; China/**NW** origin	0.31 (0.93)	8.64 (0.91)	0.048 (0.97)	0.048 (0.94)	0.069 (0.93)	4.87 (0.95)	0.18 (0.78)	27.8 (0.96)	6.39 (0.93)
P-3B, #19	plume at 2.5-3.5 km; N=61, N_{HC}=37; **SW** origin	0.21 (0.84)	10.17 (0.63)	0.038 (0.58)	0.060 (0.70)	0.095 (0.62)	8.75 (0.67)	0.50 (0.43)	39.3 (0.48)	3.72 (0.64)
	near-surface; N=195, N_{HC}=91; **NW** origin	0.27 (0.84)	6.37 (0.60)	0.044 (0.83)	0.064 (0.79)	0.052 (0.71)	1.66 (0.39)	0.66 (0.73)	20.42 (0.52)	NS

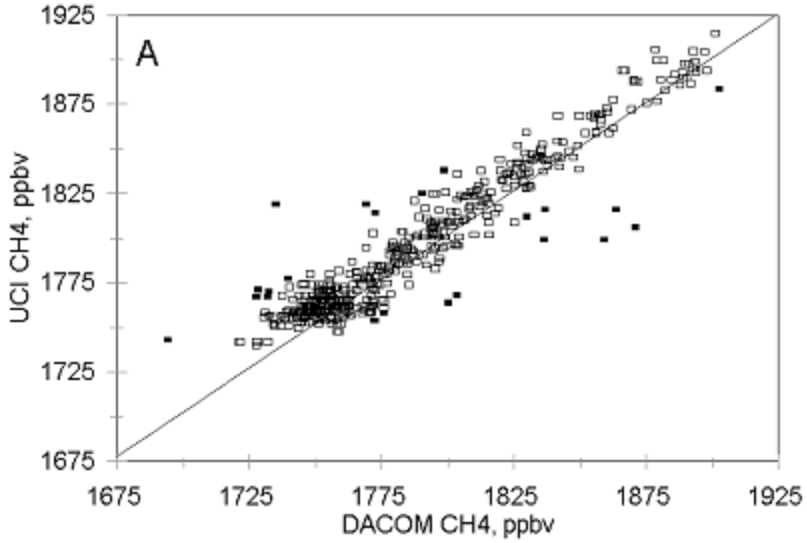
A
1925
1875
1825
1775
1725
1675
UCI CH4, ppbv
1675
1725
1775
1825
1875
1925
DACOM CH4, ppbv

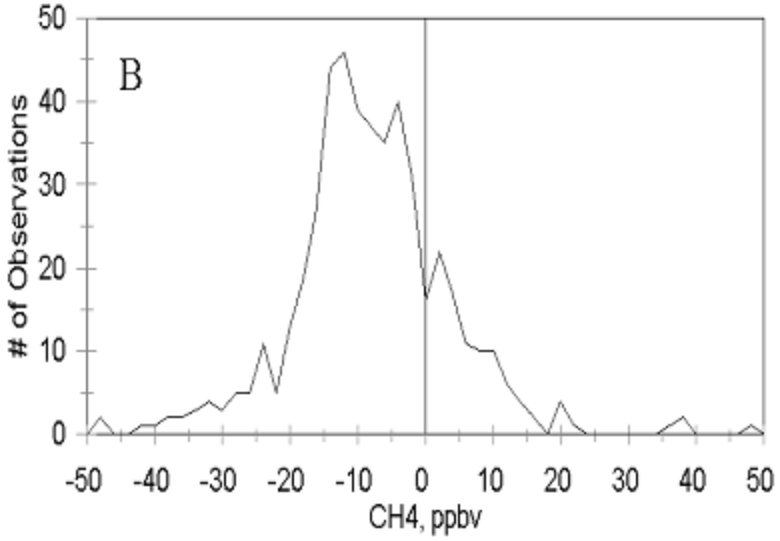
B
50
40
30
20
10
0
# of Observations
-50
-40
-30
-20
-10
0
10
20
30
40
50
CH4, ppbv

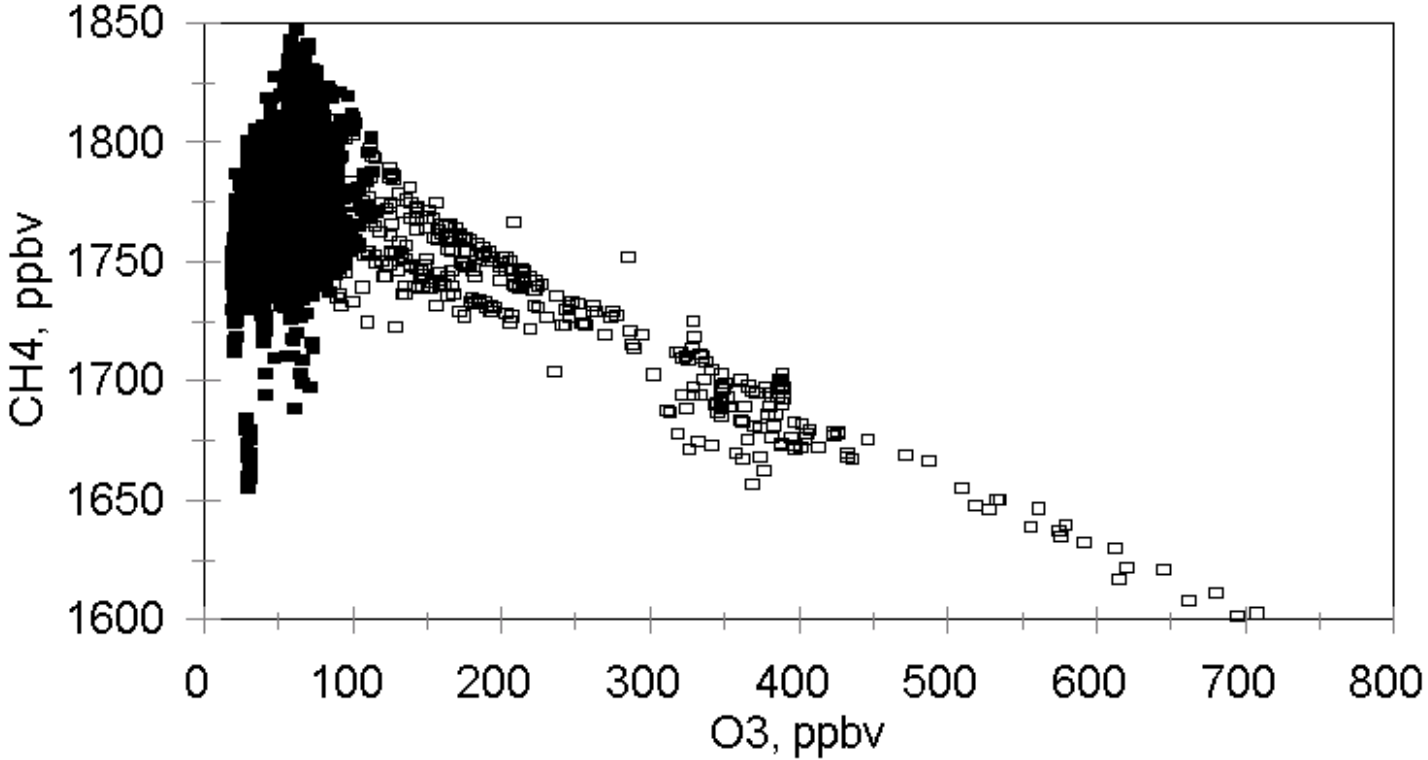
1850
1800
1750
1700
1650
1600
CH4, ppbv
0
100
200
300
400
500
600
700
800
O3, ppbv

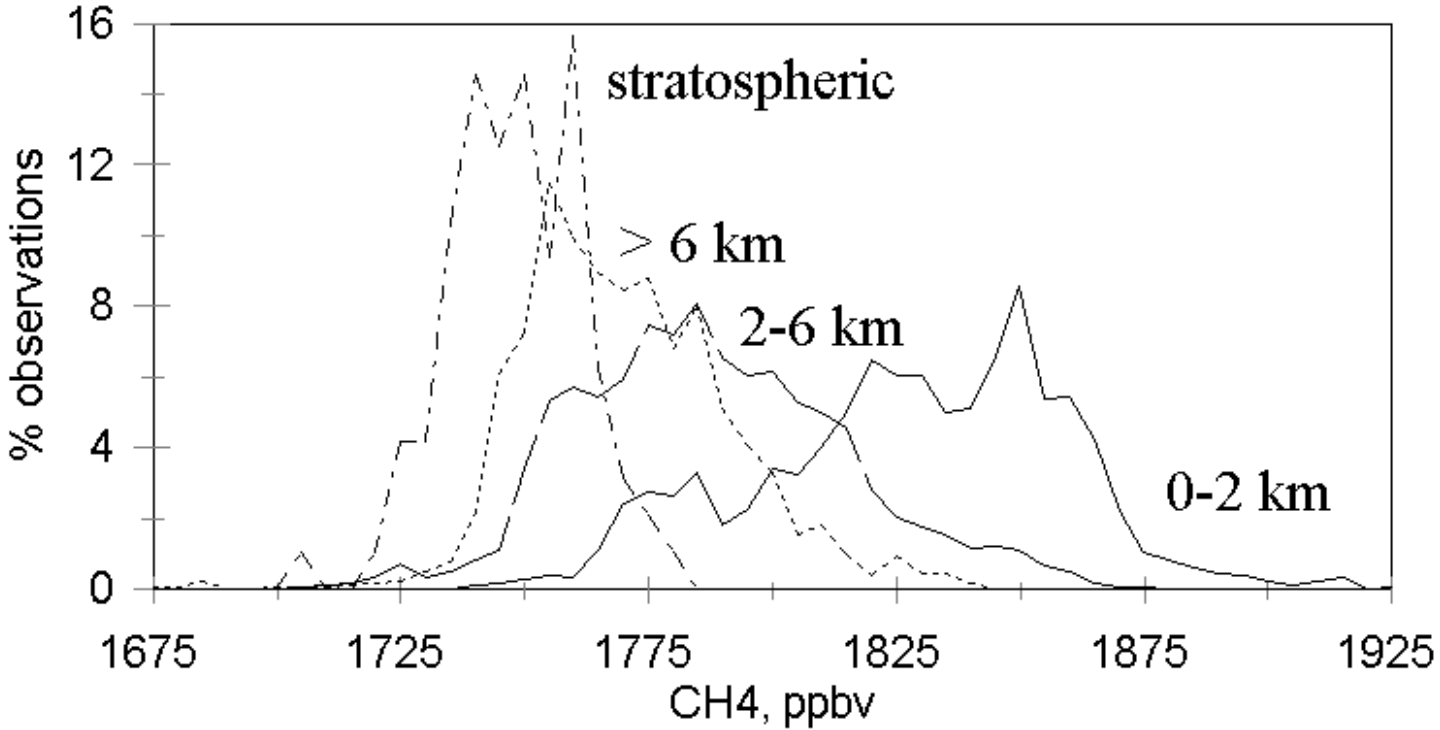
16
12
8
4
0
% observations
stratospheric
> 6 km
2-6 km
0-2 km
1675
1725
1775
1825
1875
1925
CH4, ppbv

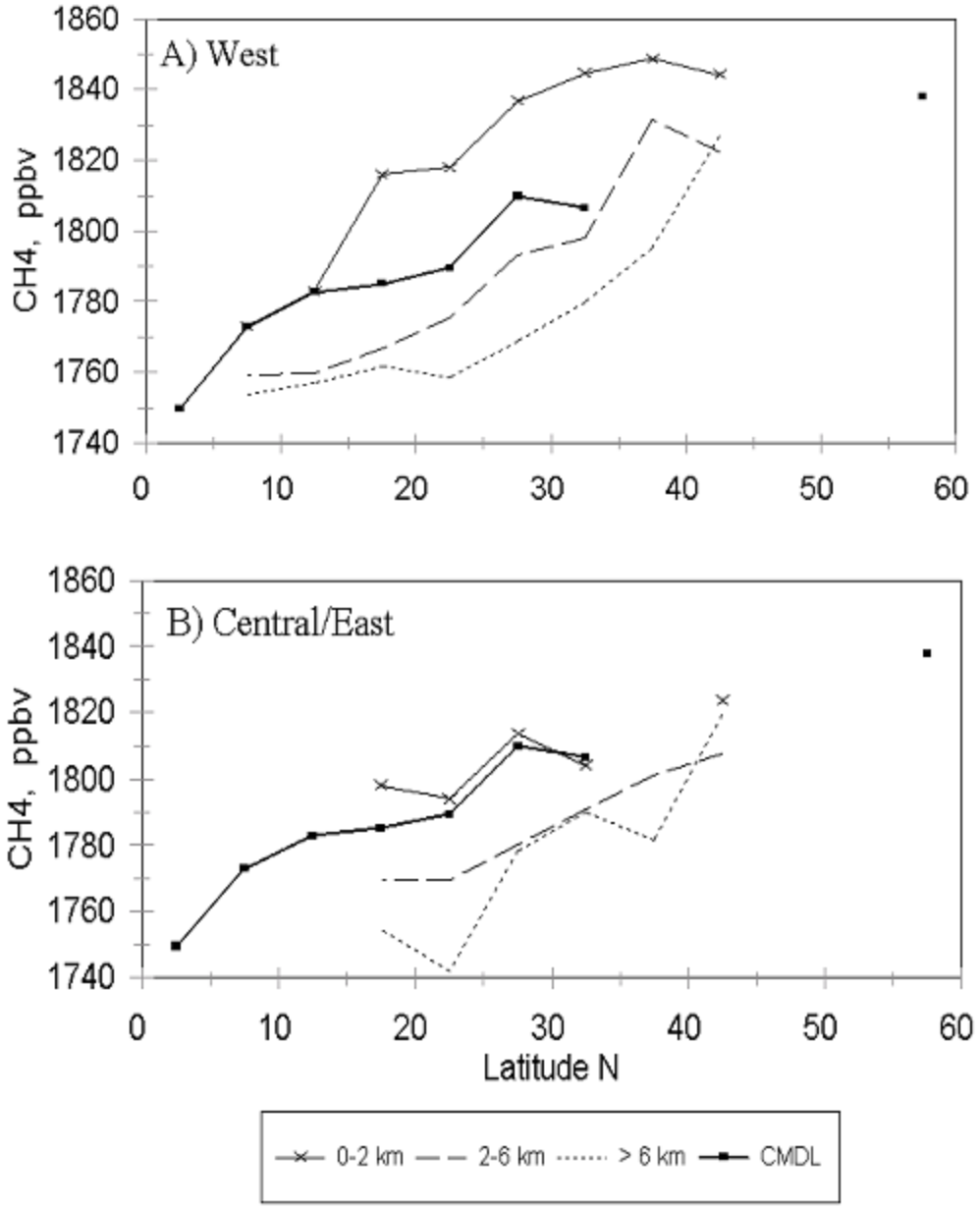
A) West
CH4, ppbv
1860
1840
1820
1800
1780
1760
1740
0
10
20
30
40
50
60

B) Central/East
CH4, ppbv
1860
1840
1820
1800
1780
1760
1740
0
10
20
30
40
50
60
Latitude N

0-2 km
2-6 km
> 6 km
CMDL

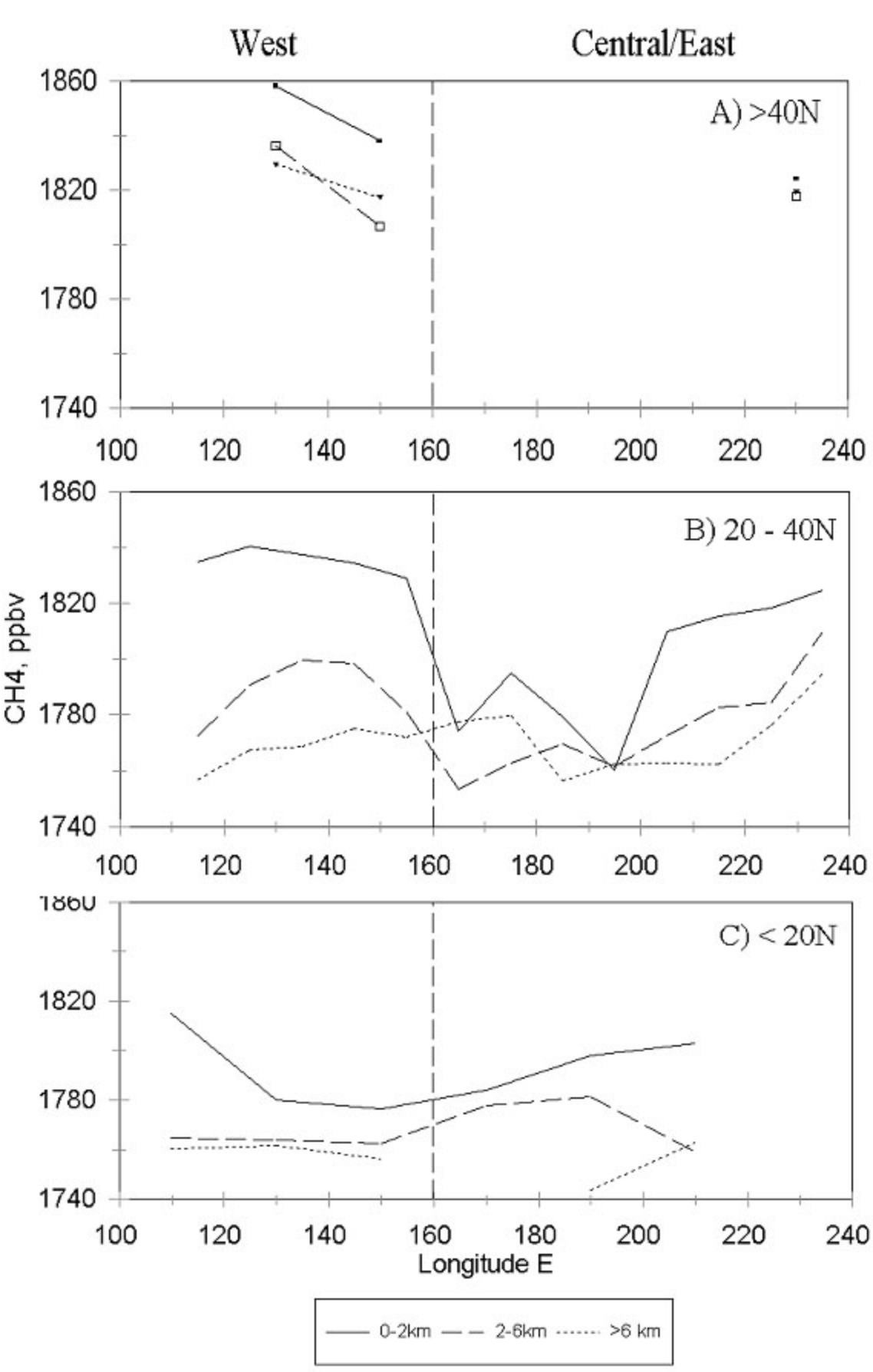
West
Central/East
A) >40N
B) 20 - 40N
C) < 20N
CH4, ppbv
Longitude E
1860
1820
1780
1740
100
120
140
160
180
200
220
240
0-2km
2-6km
>6 km

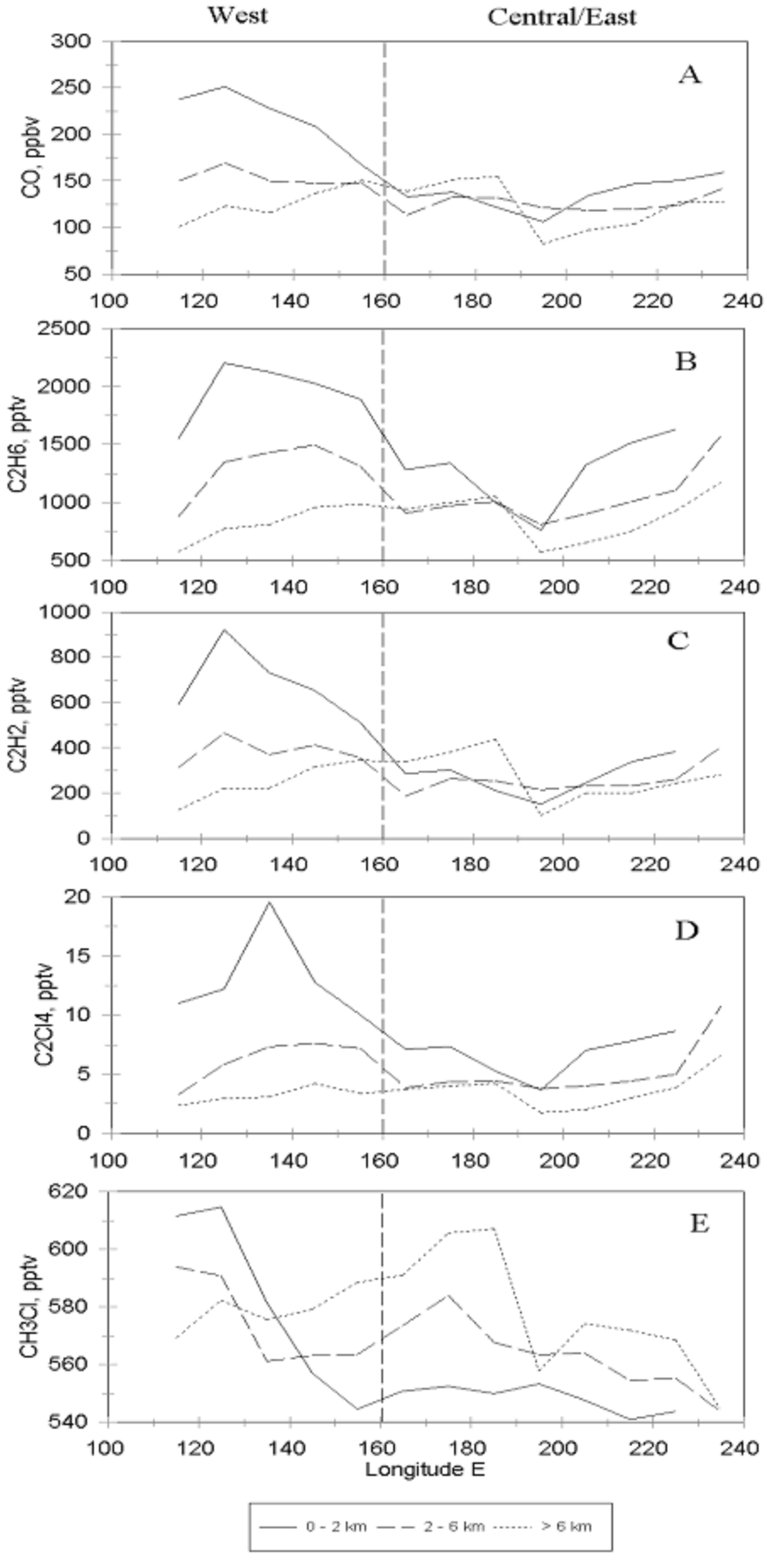
West
Central/East
A
CO, ppbv
300
250
200
150
100
50
B
C2H6, pptv
2500
2000
1500
1000
500
C
C2H2, pptv
1000
800
600
400
200
0
D
C2Cl4, pptv
20
15
10
5
0
E
CH3Cl, pptv
620
600
580
560
540
100
120
140
160
180
200
220
240
Longitude E
0 - 2 km
2 - 6 km
> 6 km

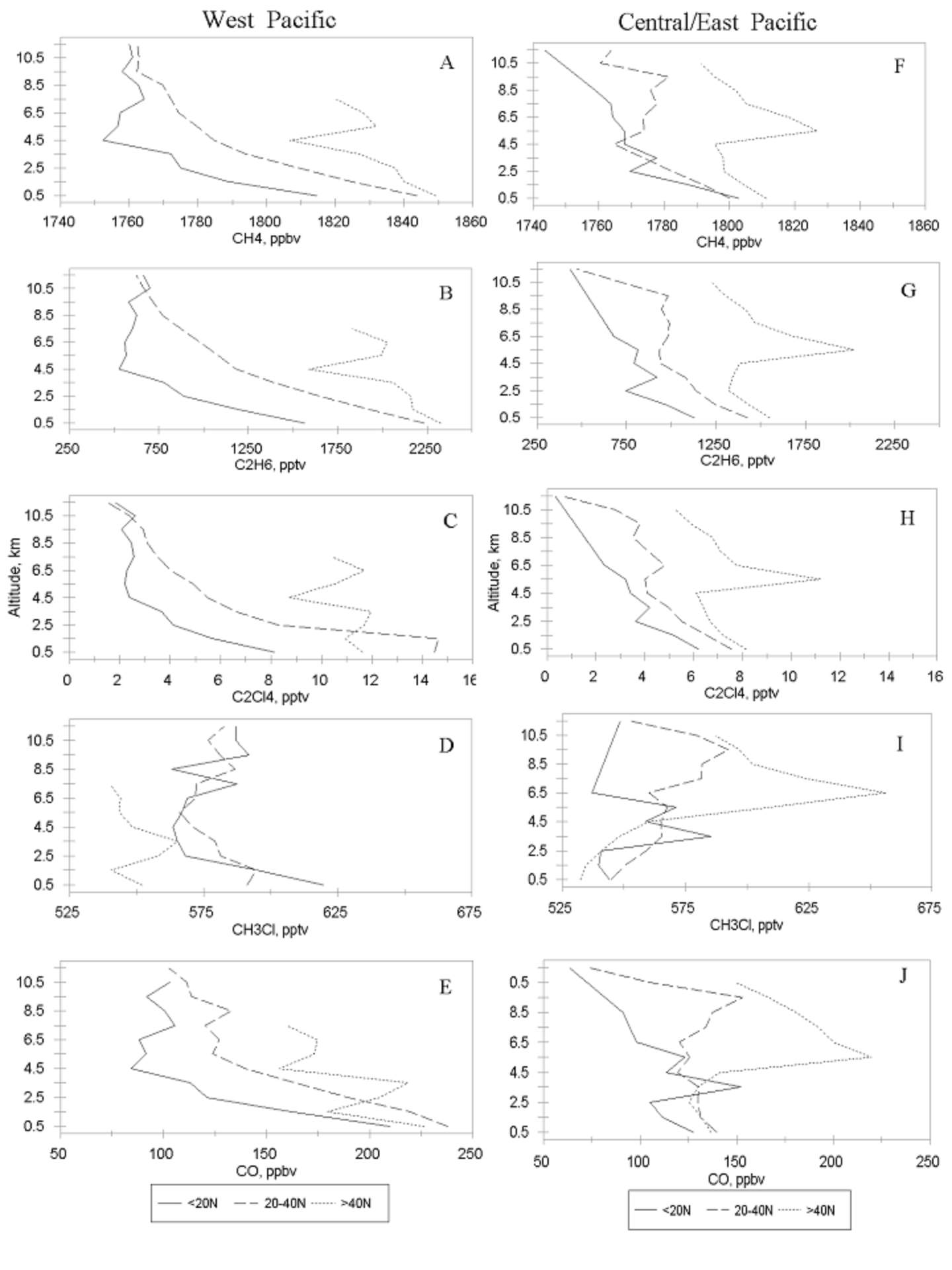
West Pacific
Central/East Pacific
A
B
C
D
E
F
G
H
I
J
Altitude, km
CH4, ppbv
C2H6, pptv
C2Cl4, pptv
CH3Cl, pptv
CO, ppbv
<20N
20-40N
>40N

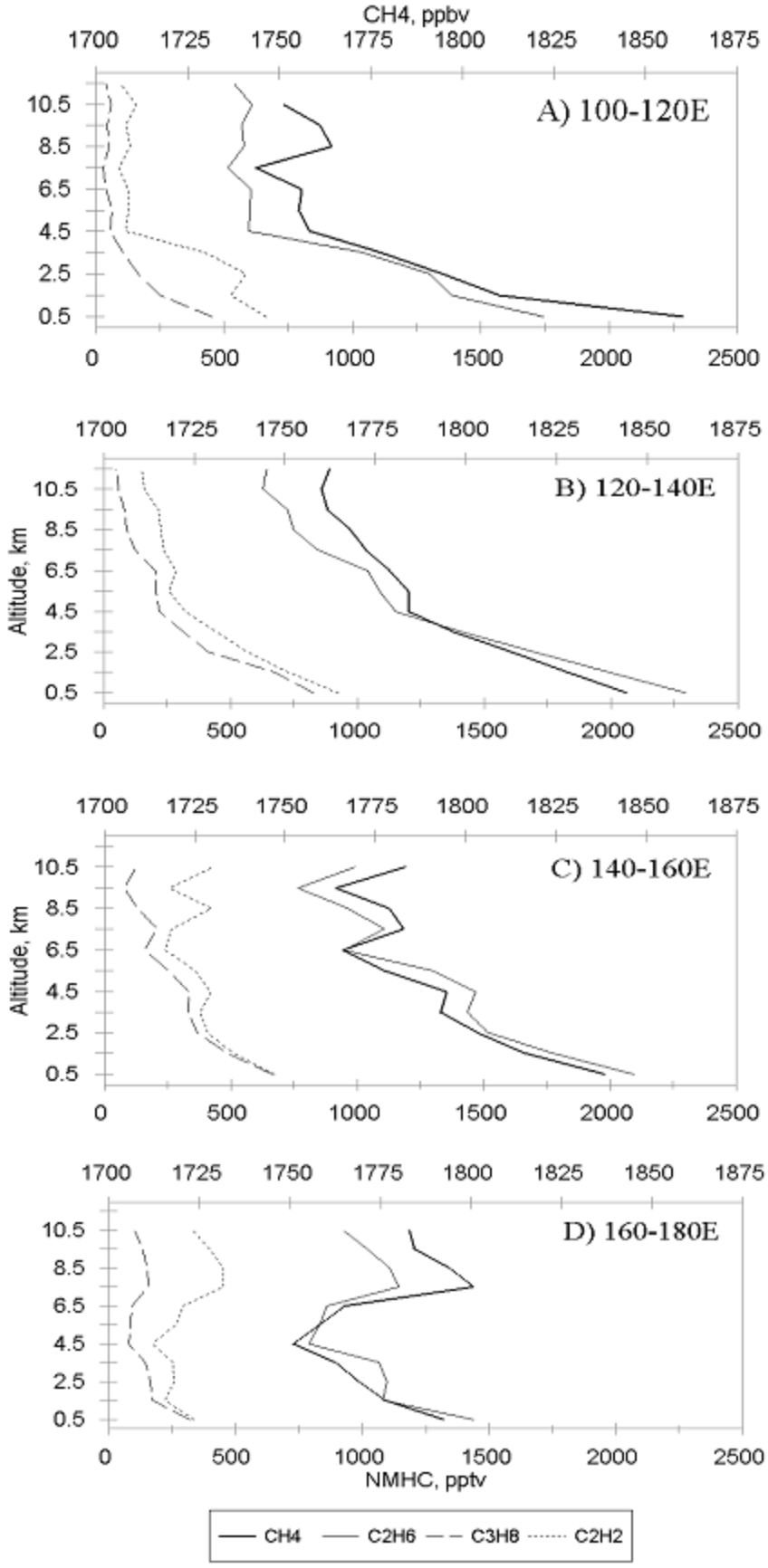
CH4, ppbv
1700 1725 1750 1775 1800 1825 1850 1875
A) 100-120E
B) 120-140E
C) 140-160E
D) 160-180E
Altitude, km
10.5 8.5 6.5 4.5 2.5 0.5
0 500 1000 1500 2000 2500
NMHC, pptv
CH4 C2H6 C3H8 C2H2

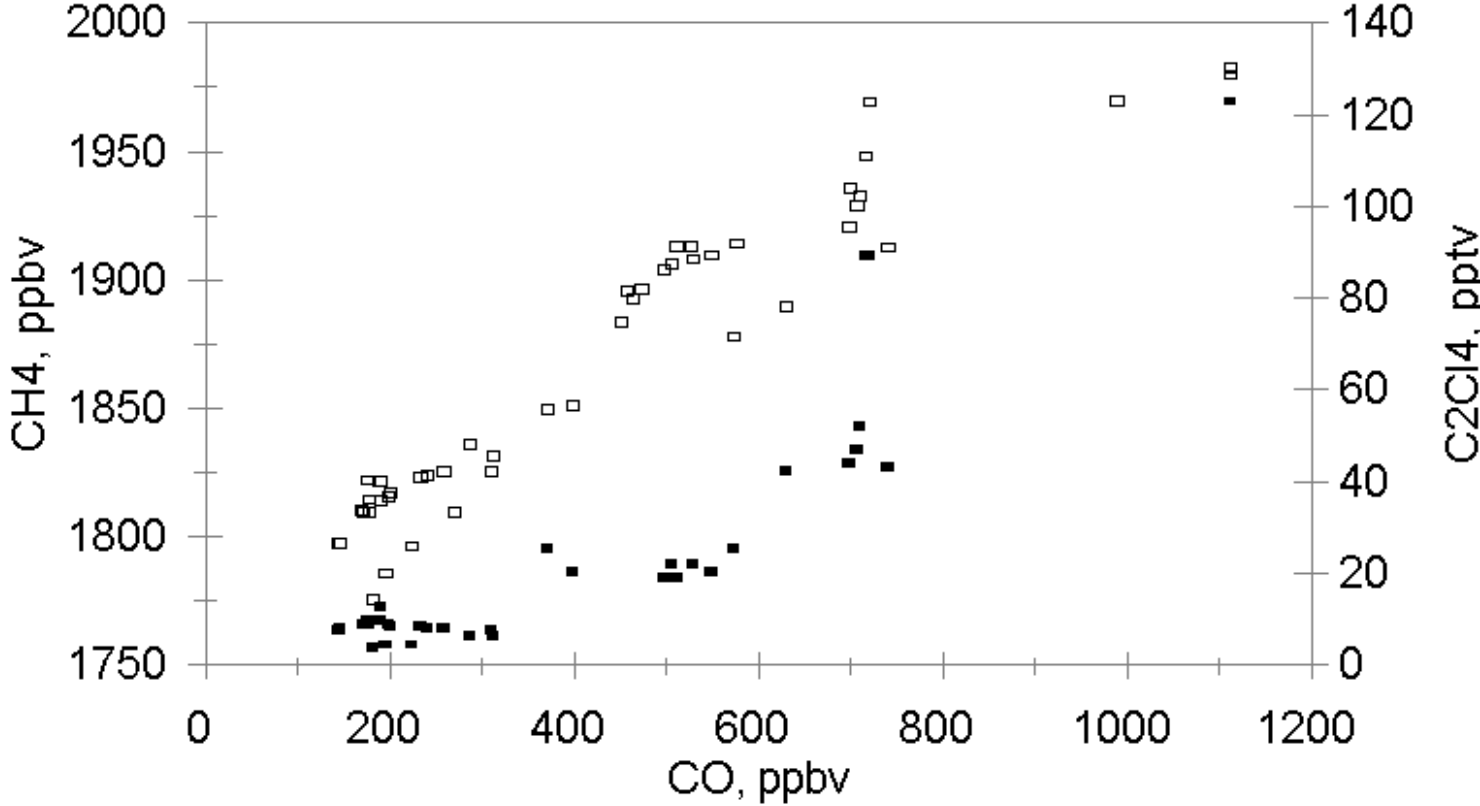
2000
1950
1900
1850
1800
1750
CH4, ppbv
140
120
100
80
60
40
20
0
C2Cl4, pptv
0
200
400
600
800
1000
1200
CO, ppbv

CH_3Cl, pptv

550

600

650

12.0

10.0

8.0

6.0

4.0

2.0

0.0

Altitude, km

1760

1800

1840

1880

CH_4, ppbv

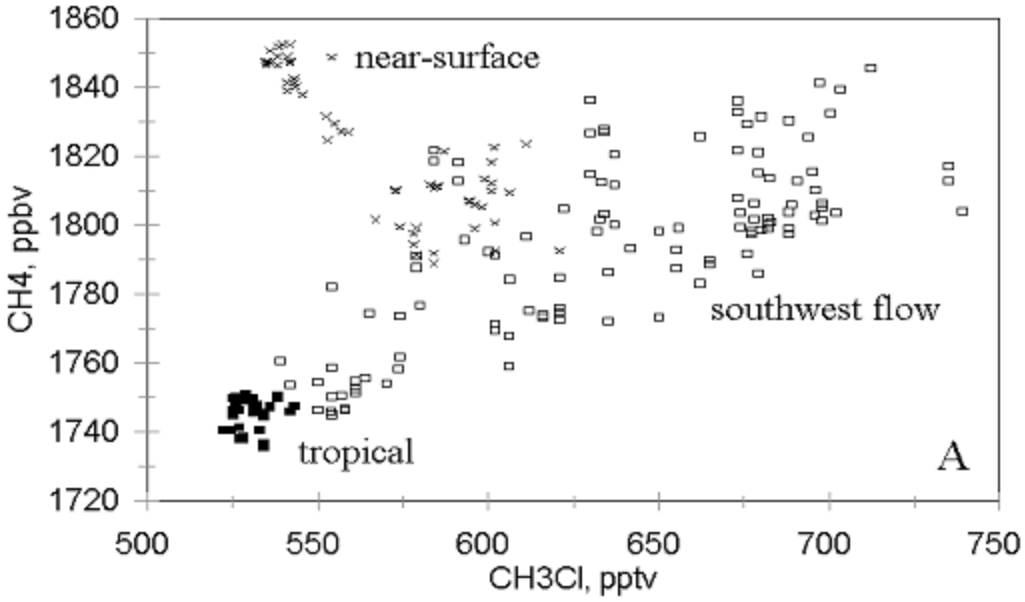
near-surface
southwest flow
tropical
A
CH4, ppbv
CH3Cl, pptv
1860
1840
1820
1800
1780
1760
1740
1720
500
550
600
650
700
750

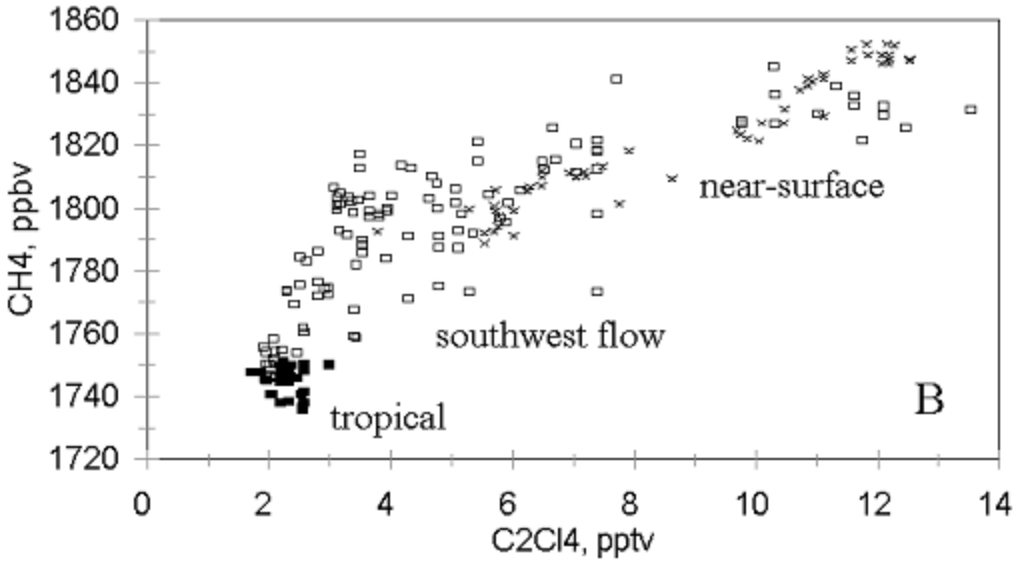
near-surface
southwest flow
tropical
B
CH4, ppbv
C2Cl4, pptv
1860
1840
1820
1800
1780
1760
1740
1720
0
2
4
6
8
10
12
14

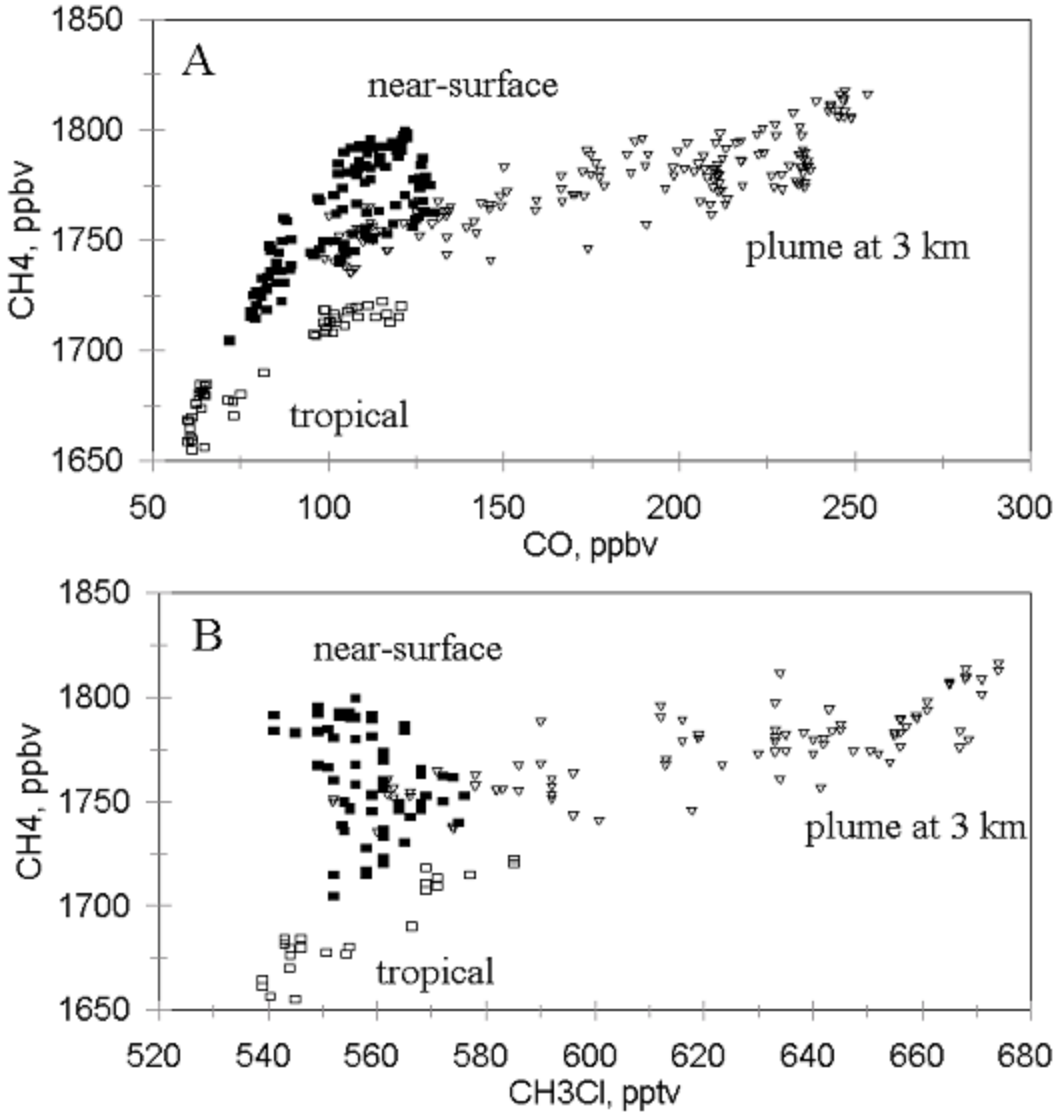
A
near-surface
plume at 3 km
tropical
CH4, ppbv
CO, ppbv
1850
1800
1750
1700
1650
50
100
150
200
250
300
B
near-surface
plume at 3 km
tropical
CH4, ppbv
CH3Cl, pptv
1850
1800
1750
1700
1650
520
540
560
580
600
620
640
660
680

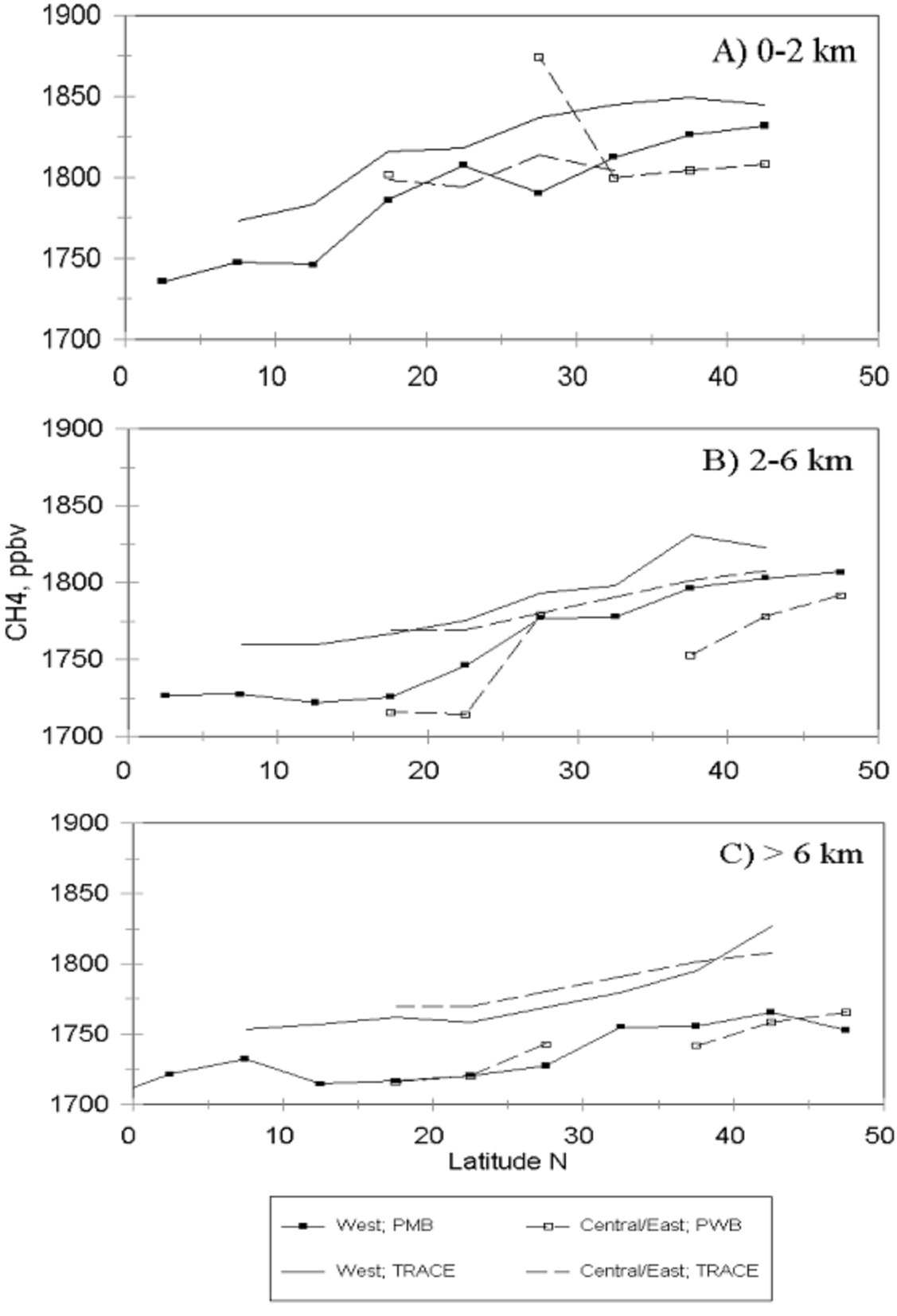
A) 0-2 km
B) 2-6 km
C) > 6 km
CH4, ppbv
Latitude N
1900
1850
1800
1750
1700
0
10
20
30
40
50
West; PMB
Central/East; PWB
West; TRACE
Central/East; TRACE

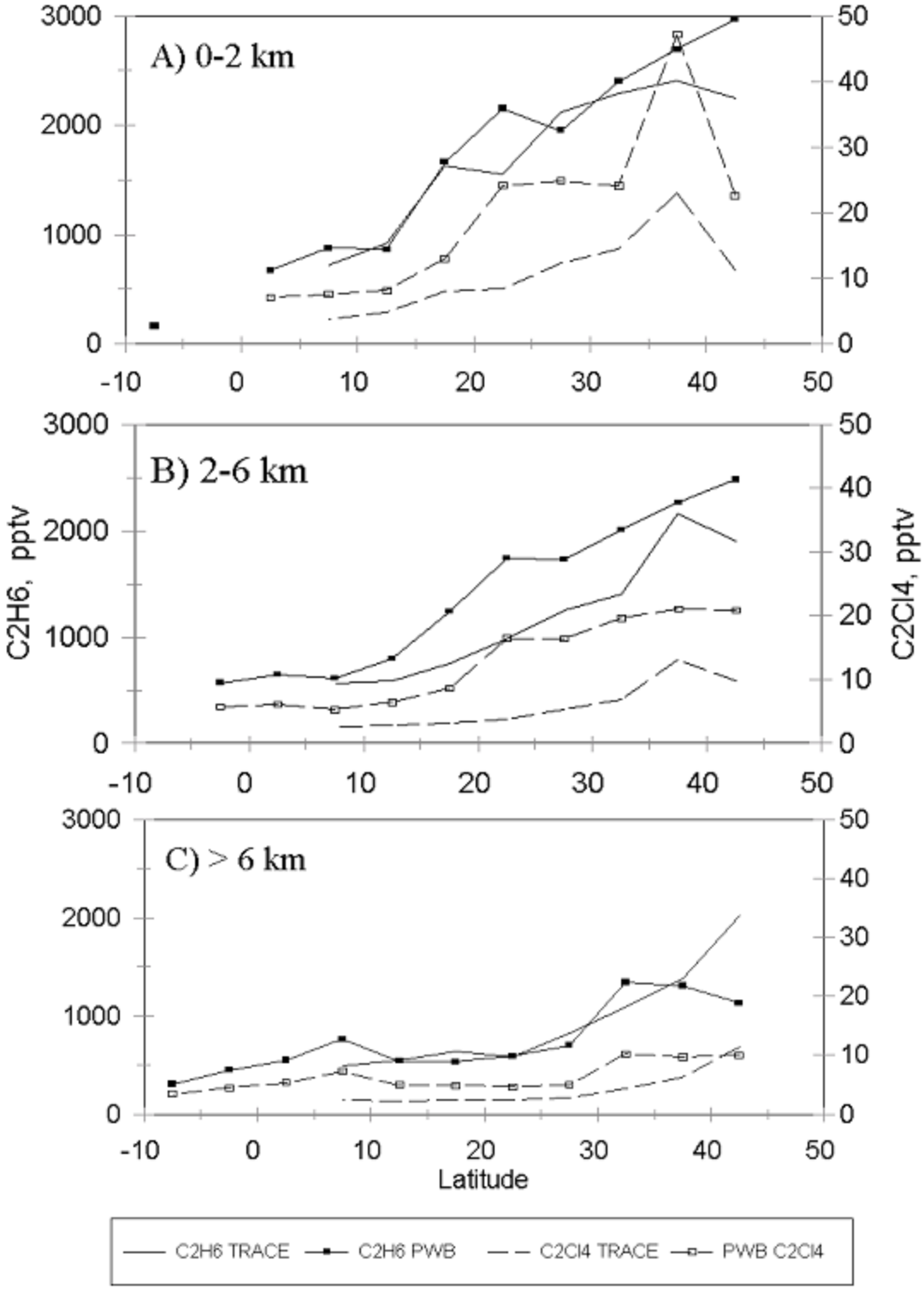
A) 0-2 km
B) 2-6 km
C) > 6 km
C2H6, pptv
C2Cl4, pptv
Latitude
C2H6 TRACE
C2H6 PWB
C2Cl4 TRACE
PWB C2Cl4

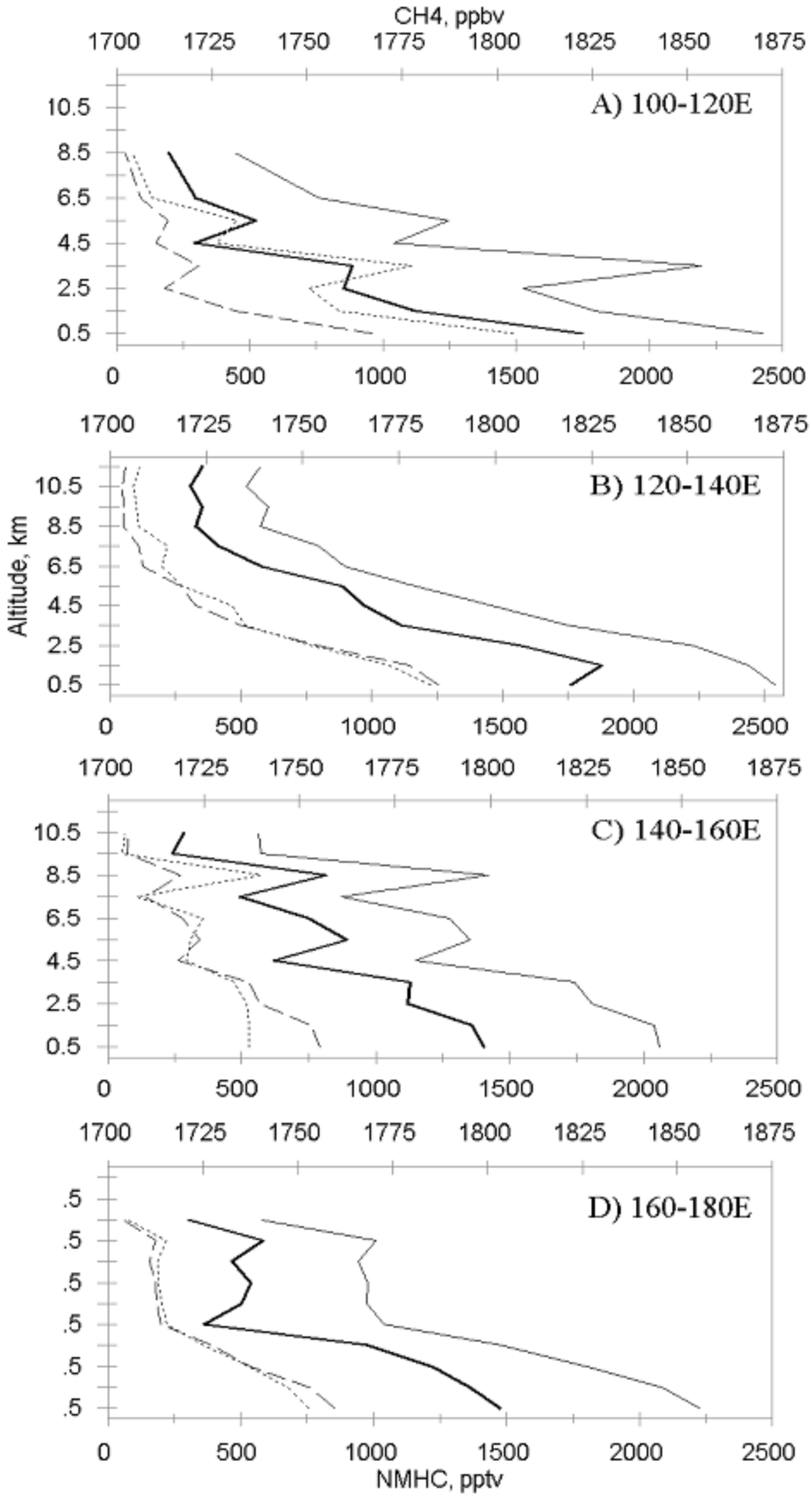
CH4, ppbv
1700 1725 1750 1775 1800 1825 1850 1875
A) 100-120E
B) 120-140E
C) 140-160E
D) 160-180E
Altitude, km
10.5
8.5
6.5
4.5
2.5
0.5
0 500 1000 1500 2000 2500
NMHC, pptv
CH4
C2H6
C3H8
C2H2

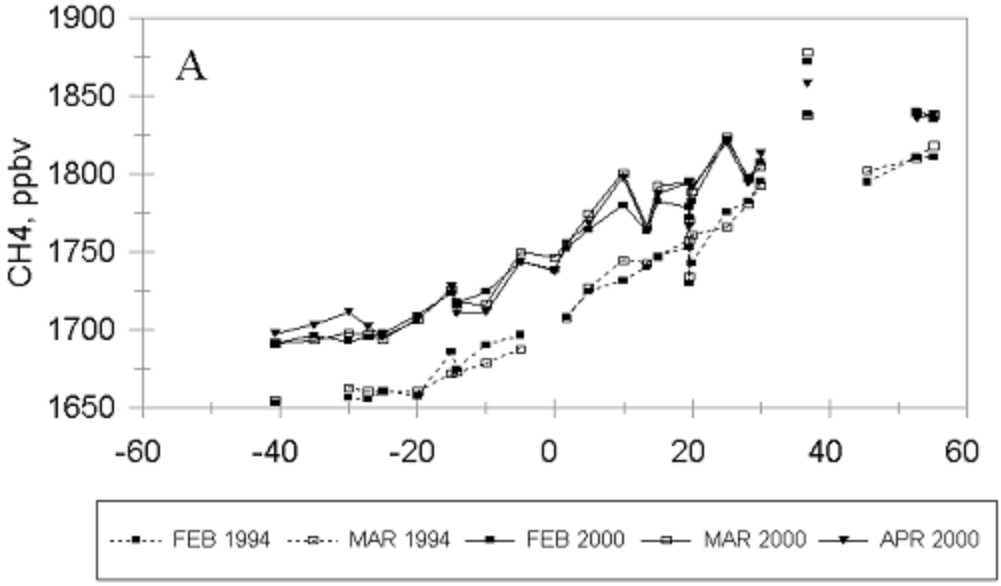
A
CH4, ppbv
1900
1850
1800
1750
1700
1650
-60
-40
-20
0
20
40
60
FEB 1994
MAR 1994
FEB 2000
MAR 2000
APR 2000

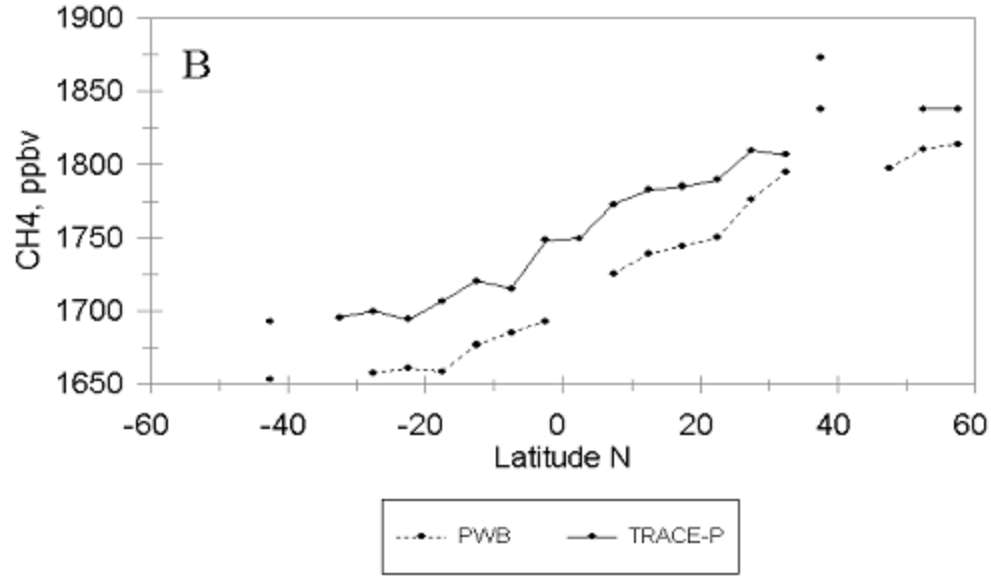
B
CH4, ppbv
1900
1850
1800
1750
1700
1650
-60
-40
-20
0
20
40
60
Latitude N
PWB
TRACE-P

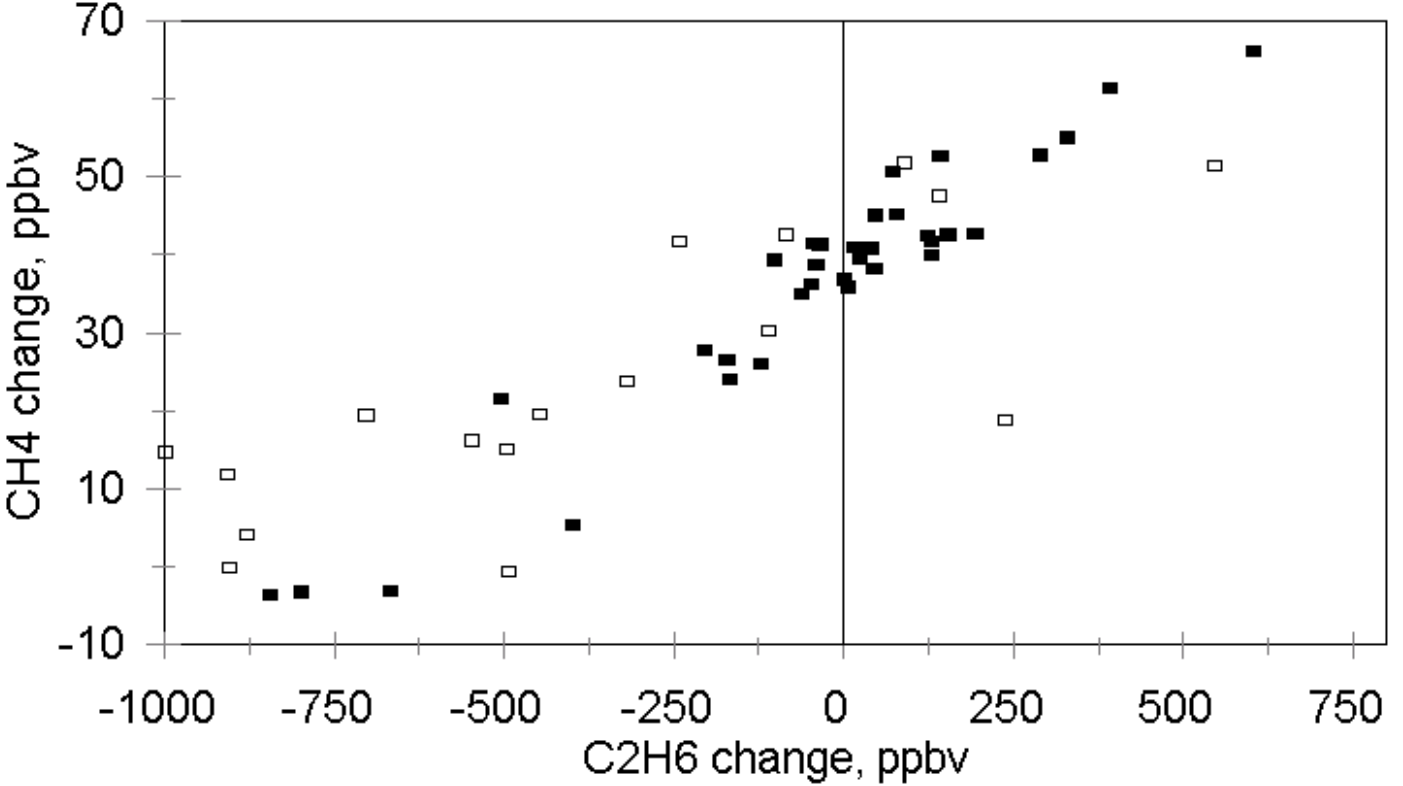
70
50
30
10
-10
CH4 change, ppbv
-1000
-750
-500
-250
0
250
500
750
C2H6 change, ppbv

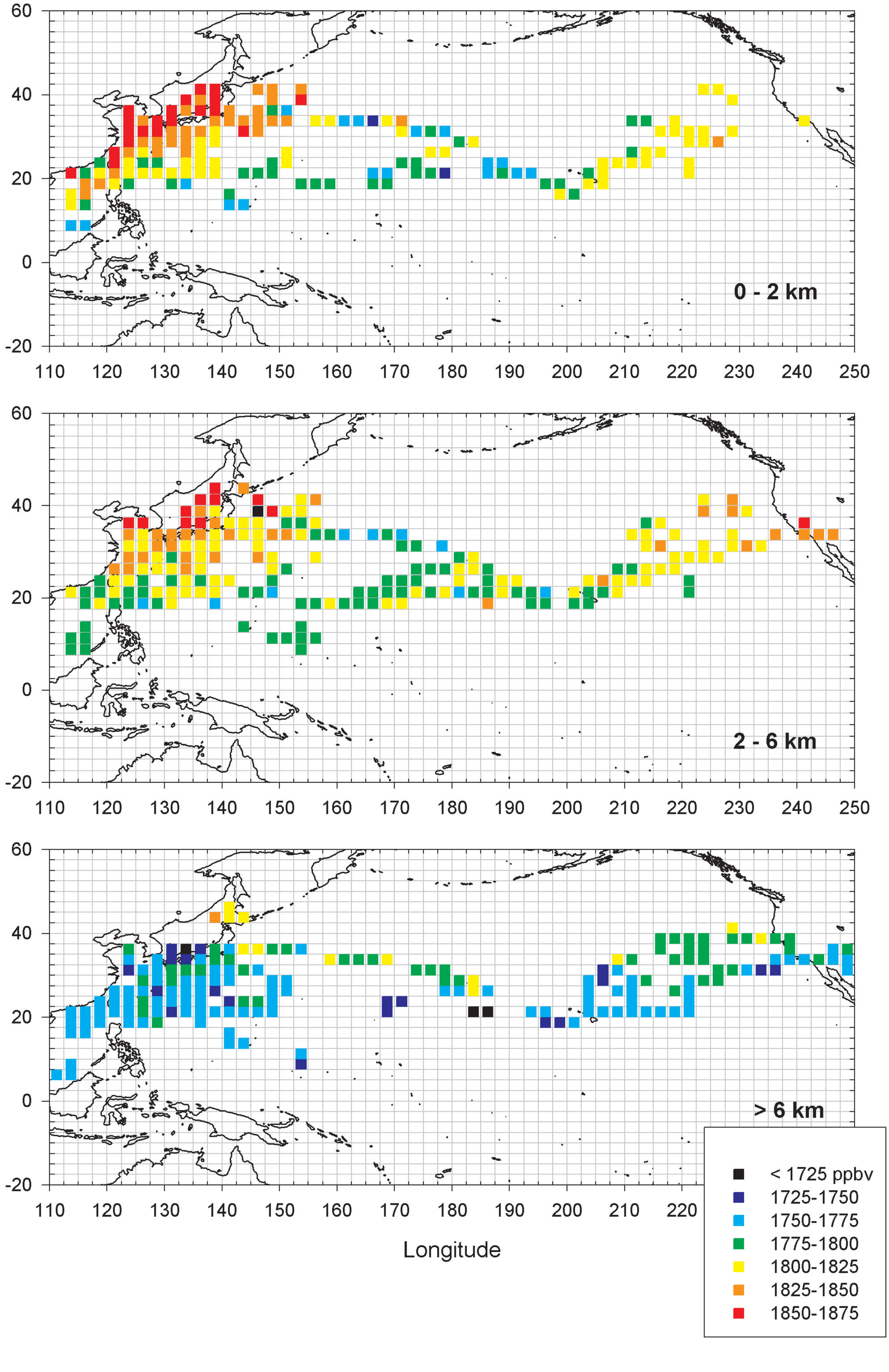
0 - 2 km
2 - 6 km
> 6 km
Latitude
Longitude
60
40
20
0
-20
110
120
130
140
150
160
170
180
190
200
210
220
230
240
250
< 1725 ppbv
1725-1750
1750-1775
1775-1800
1800-1825
1825-1850
1850-1875

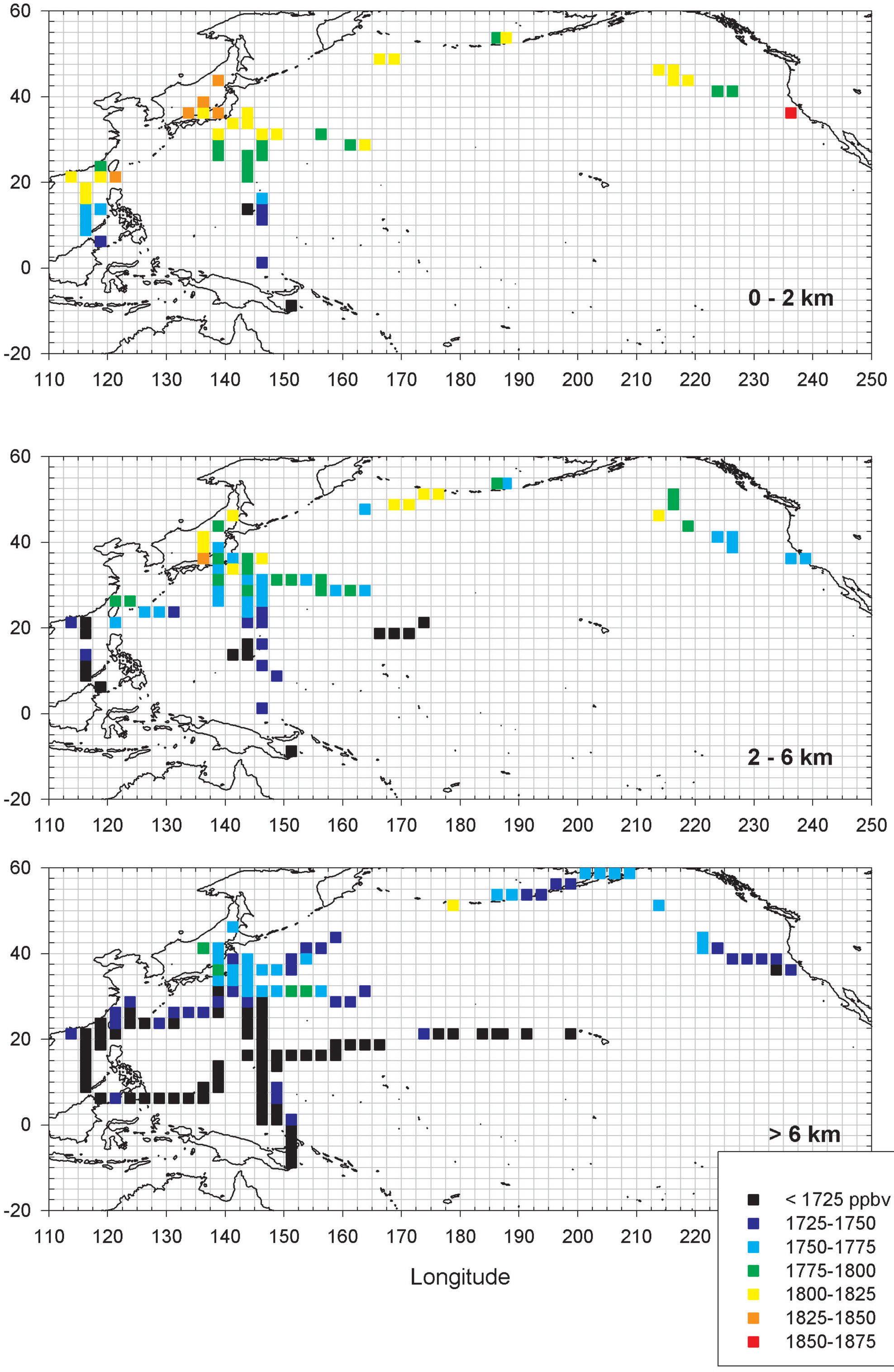
0 - 2 km
2 - 6 km
> 6 km
Latitude
Longitude
60
40
20
0
-20
110
120
130
140
150
160
170
180
190
200
210
220
230
240
250
< 1725 ppbv
1725-1750
1750-1775
1775-1800
1800-1825
1825-1850
1850-1875